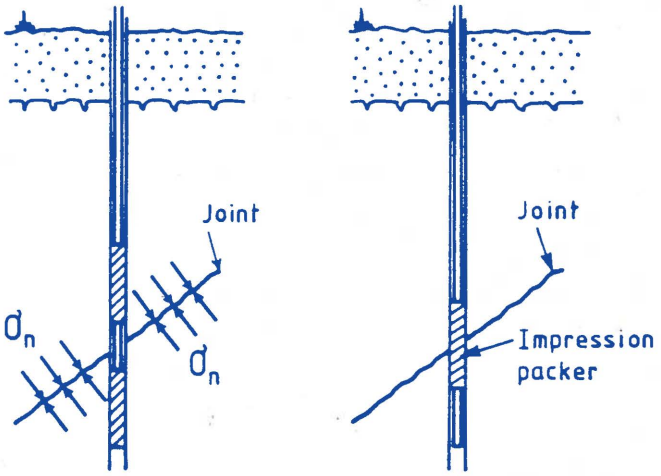
BeFo



A comparison of Hydraulic Measuring Techniques for Borehole Rock Stress Measurements

Christer Ljunggren
Bjarni Bjarnason

Stiftelsen Bergteknisk Forskning – BeFo
Swedish Rock Engineering Research Foundation

BeFo 211:1/90

A Comparison of Hydraulic Measuring Techniques for Borehole Rock Stress Measurements

Jämförande bergspänningsmätningar i borrhål med hydrauliska metoder

Christer Ljunggren
Bjarni Bjarnason

Division of Rock Mechanics,
Luleå University of Technology

Stiftelsen Bergteknisk Forskning – BeFo
Swedish Rock Engineering Research Foundation
Stockholm 1990

FÖRORD

Projektet "Bergspänningars roll i bergmekaniska beräkningar" i BeFos ramprogram 87-90 syftar till bättre teknik för bergspänningsmätning och värdering av bergspänningsdata i samband med bergmekaniska beräkningar.

Inom ramen för detta projekt har BeFo bidragit som delfinansiär av projektet "A comparison of hydraulic measuring techniques for borehole rock stress measurements" vid Tekniska Högskolan i Luleå, med syftet att stödja utvecklingen av nya mätmetoder som till måttliga kostnader kan ge tillförlitliga data om bergspänningsförhållanden. Projektet har även fått stöd från Naturvetenskapliga Forskningsrådet.

Föreliggande rapport redovisar jämförande mätningar och vissa svårigheter som är förknippade med den nya s.k. HTPF-metoden, vilken dock innehåller fördelar i vissa speciella tillämpnigar.

Tomas Franzén

SAMMANFATTNING

Rapporten redovisar resultaten från bergspänningsmätningar i det vertikala, 508 m djupa borrhålet på högskoleområdet i Luleå. Mätningarna utfördes under vintern 88/89 och våren 1989. Bergspänningarna bestämdes med två hydrauliska metoder; hydraulisk spräckning och hydrauliska tester på befintliga sprickor (HTPF). De primära ändamålen med studien var; (i) att jämföra de båda metoderna med varandra, både vad gäller fältarbete och erhållen information om spänningssituationen in-situ, (ii) att erhålla pålitlig information om spänningsmagnituderna och orienteringarna på spänningarna i området.

Spänningsmätningarna utfördes från ca 40 m ner till 500 m djup. Den dominerande bergarten i borrhålet (LuH) är migmatiserad gnejs med ett flertal zoner av granit och pegmatit.

Resultaten från hydraulisk spräckning och den tvådimensionella HTPF-analysen visar att den minsta horisontella spänningen ökar linjärt med djupet och når en magnitud av 11.5 MPa på 400 m djup. Den största horisontella spänningen är 21.5 MPa på 400 m djup. Den tredimensionella HTPF-analysen visade sig vara mycket känslig för ingångsvärdena. Analysen indikerar dock att huvudspänningarna är orienterade i vertikal- och horisontalplanen.

Den största horisontella spänningen har orienteringen N40°W enligt den tvådimensionella HTPF-analysen. Från mätningarna med hydraulisk spräckning erhölls en orientering av N-S. De hydrauliskt inducerade sprickorna har dock sannolikt följt de brant stupande foliationsplanen i bergmassan, vilka stryker i en nord-sydlig riktning, och förkastas därför i detta fall som metod att bestämma orienteringen av största horisontella spänningen.

De båda metoderna att bestämma bergspänningar nyttjar identisk utrustning, men HTPF-metoden är mer tidskrävande. De främsta orsakerna till detta är: (i) Att lokalisera en naturlig, isolerad spricka är mer tidskrävande jämfört med att lokalisera

sprickfria sektioner i borrhålet, (ii) pumptesterna för HTPF-metoden utförs med ett lägre vätskeflöde och därigenom tas mer tid i anspråk.

Hydraulisk spräckning rekommenderas för att bestämma berg-spänningarna om det inte finns några tecken som tyder på att berget är anisotropt, samt om någon av huvudspänningarna är vertikalt orienterad.

TABLE OF CONTENTS

		Page
	SUMMARY	
1	INTRODUCTION	1
2	TEST SITE DESCRIPTION	2
2.1	Location and topography	2
2.2	Geology	2
2.3	Borehole LuH	3
2.4	Mechanical properties of the rock	3
3	FIELD EQUIPMENT	6
3.1	Field instrumentation	6
3.2	Field work	9
4	HYDRAULIC FRACTURING	10
4.1	Stress calculations	10
4.1.1	Classical theory	10
4.1.2	Theory using the Hoek and Brown failure criterion	12
4.2	Data analysis	14
4.2.1	Breakdown pressures	14
4.2.2	Shut-in pressures	14
4.2.3	Tensile strength	15
4.3	Results and interpretation	17
4.3.1	Stress magnitudes	19
4.3.2	Stress orientations	23
4.3.3	Interpretation	24
5	HYDRAULIC TESTS ON PREEXISTING FRACTURES - HTPF	28
5.1	Introduction	28
5.2	Theory	28
5.3	Modelling of the stress state	30
5.3.1	Three-dimensional model	30
5.3.2	Two-dimensional model	31
5.4	Results	32

Page

5.4.1 Two-dimensional state of stress 34
5.4.2 Three-dimensional state of stress 38

6 COMPARISON OF RESULTS 42
6.1 Orientations 43
6.2 Magnitudes 44

7 DISCUSSION AND FUTURE DEVELOPMENT 46

8 CONCLUSIONS 49

9 ACKNOWLEDGEMENTS 51

10 REFERENCES 52

APPENDIX 1
APPENDIX 2
APPENDIX 3

SUMMARY

This report presents the results from rock stress measurements conducted in the vertical, 508 m deep LuH borehole, located at the campus of Luleå University of Technology. The measurements were conducted during the winter 88/89 and spring 1989. The rock stress measurements were done by use of two hydraulic testing methods; hydraulic fracturing and hydraulic tests on preexisting fractures (HTPF). The primary objectives of this study were; (i) to compare the methods with each other, both with regard to field work and obtained information on the far field stress situation, (ii) to obtain reliable information on the stress magnitudes and stress orientations in the area.

The stress measurements were conducted from 40 m depth down to 500 m depth. The principal rock type in corehole LuH is migmatized gneiss with several zones of granite and pegmatite.

The results from the hydraulic fracturing and two-dimensional HTPF stress analysis show that the minimum horizontal stress increases linearly with depth and reaches a magnitude of about 11.5 MPa at 400 m depth. For the maximum horizontal stress we obtain a magnitude of about 21.5 MPa at 400 m depth. The three-dimensional HTPF stress analysis showed to be very sensitive to the input data. The 3-D analysis, however, indicates that the principal stresses are oriented in the vertical and horizontal planes.

The orientation of the maximum horizontal stress, as determined from the 2-D HTPF analysis, is N40°W. The average orientation of the hydraulic fracturing induced fractures is N-S. The hydrofractures, however, are belived to have lined up with the existing, steep dipping planes of foliation in the rock mass that strike N-S, and are therefore rejected for the determination of the orientation of the maximum horizontal stress.

The stress measurement methods use identical equipment for

testing. The HTPF method is though more time consuming, and the main reasons for that are: (i) more time is needed to locate isolated joints compared to locate fracture-free sections in the borehole wall, (ii) the pump tests are done with a lower flow rate in the HTPF tests.

Hydraulic fracturing is recommended to be used to determine the horizontal stress field if there are no reasons to belive that the rock is anisotropic and if one of the principal stresses is vertically oriented.

1 INTRODUCTION

During the autumn 1986 a 508 m deep borehole was drilled at the university campus just outside the rock mechanics laboratory. In 1987 a new rock mechanics laboratory was built where the borehole had been drilled. Since then the borehole is available indoor all the year, independent of weather conditions.

During stress measurements in 1986 at Gideå the HTPF (Hydraulic Tests on Preexisting Fractures) method was tested for the first time in the Nordic countries, Ljunggren and Raillard (1986). These tests showed promising results and more comprehensive field experiments by use of the HTPF method were therefore suggested to be conducted.

It was decided to test the method in the deep borehole (borehole LuH) at the university and compare field procedures as well as obtained results with the conventional hydraulic fracturing technique. At the same time the measurements would give important information on the stress field in the area. Luleå is a white spot on the rock stress map. No rock stress measurements have been conducted in eastern Norrbotten within an area of about 150 km radius from Luleå.

During the winter 1988/1989 complete field measurements were done with both methods, then followed by separate evaluation of the results for each method and finally a comparison of obtained results.

2 TEST SITE DESCRIPTION

2.1 Location and topography

Luleå is situated in the southeast part of the Norrbotten county at the coast of Gulf of Bothnia. The coastal areas of this region reflect among the highest isostatic land uplift observed in Sweden, being 10 mm/year. The topography in the area is generally flat. Just south of Luleå city, at Bälingeberget, evidence of the highest coastlines can be observed.

2.2 Geology

The area is situated at the border of what now is believed to have been an Archean continent of craton, which today is considerably reshaped by geological processes through time and partly overlain by younger supracrustals and intrusions, Lilljequist (1980). The nearest areas of proven Archean age extend south of Kemi in Finland and along the Swedish-Finnish border on the west side of the Torne river, Fig. 2.1.

Migmatized gneiss, mainly of sedimentary origin, is found east of the borehole and is being ranked equal with the marine sedimentary gneisses further south, Fig. 2.1. The border is probably of tectonical origin, created by block movement. Rock types belonging to the Haparanda series diorites-quartsdiorites-granites are found west of the borehole. Exposures of gneissic intermediate and basic vulcanites can be seen in the vicinity of the borehole. Further, Lina granite is present in surrounding areas.

The borehole penetrates soil to a depth of 6.5 m and solid bedrock is obtained at 8 m depth. The principal rock type in borehole LuH is migmatized gneiss. Steep planes of foliation striking N-S is found in the gneiss, Röshoff and Norin (1982) and Ludvig (1981). Two crushed zones are encountered in the

hole, one between 150 m - 170 m and one between 346 m - 350 m depth. Both crushed zones contains breccias and mylonites indicating that movement has occured. The borehole geology also includes several zones of granite and pegmatite.

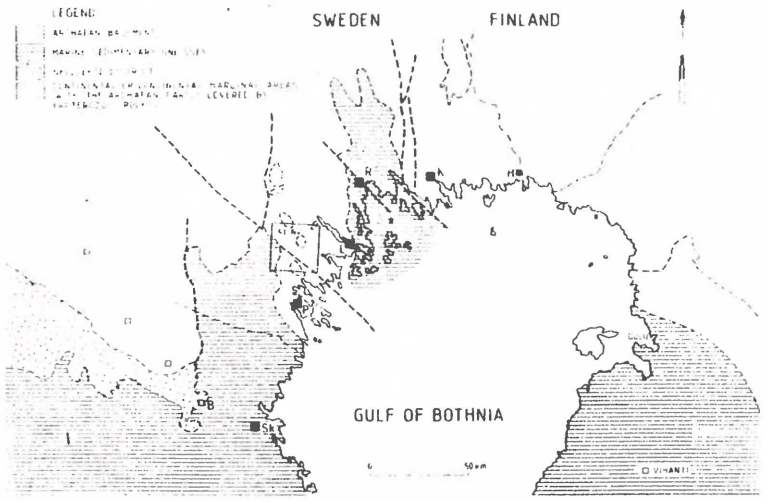


Fig. 2.1. Distribution of major geological rock units around the Gulf of Bothnia. H = Haparanda, K = Kalix, R = Råneå, L = Luleå, P = Piteå, Sk = Skellefteå and B = Boliden. (After Lilljequist, 1980)

2.3 Borehole LuH

The borehole is core drilled to the bottom at 508 m depth and is vertically orientated. The deviation from the vertical is at maximum 2° and the diameter of the hole is 56 mm. This is the only deep core drilled borehole in an area with about 150 km radius from Luleå.

2.4 Mechanical properties of the rock

A comprehensive study of the mechanical properties of the rock from borehole LuH has been conducted. The results have partly

been presented in Thorsager (1987). Some of the tests conducted and parameters studied are summarized below.

The rock material in borehole LuH has undergone the following tests:

- Hydraulic fracturing on core samples; Tensile strength, (T) of the rock
- Uniaxial compression tests; Static Young's modulus, (E_s), static Poisson's ratio, (ν_s) and the uniaxial compressive strength, (σ_c)
- triaxial compression tests; Young's modulus (E), Poisson's ratio, (ν) and the compressive strength (σ_{1c})
- Brazilian disc tests; Tensile strength, (T)

The laboratory tests were conducted on gneiss and granite. The unconfined compressive strength for migmatitic gneiss was 171 MPa, while its tensile strength determined by Brazilian disc tests was 12 MPa. The compressive and tensile strength values for granite was 242 MPa and 15 MPa, respectively. The compressive strength value for the granite is rather high, while the tensile strength values for both rock types are typical for crystalline rocks.

As part of the evaluation of intact rock strength, failure envelopes were constructed for both rock types investigated, Figs. 2.2 and 2.3, and the empirical constant m incorporated in the Hoek and Brown failure criterion was then determined.

The uniaxial compressive strength, σ_c, obtained from the application of the Hoek and Brown criterion to the laboratory data was 260 MPa and 161 MPa for the granite and the gneiss, respectively. The obtained m and σ_c values were applied to back

calculate the tensile strength values, which resulted in 14.8 MPa for the granite and 10.8 MPa for the gneiss.

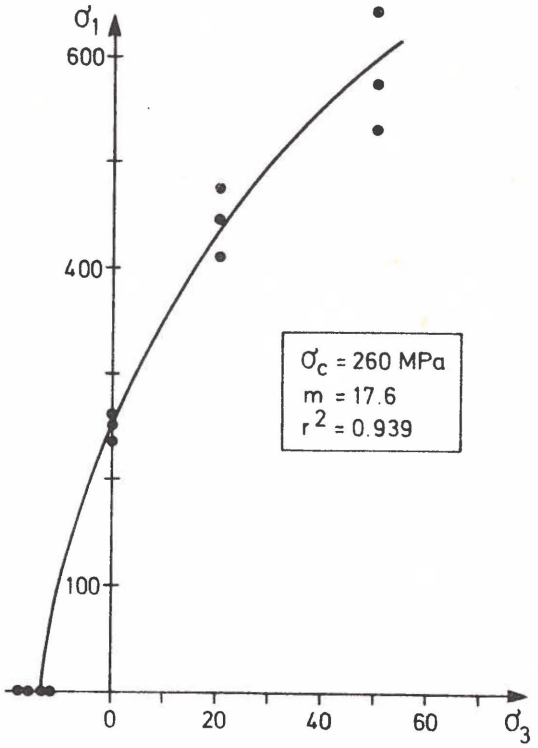


Fig. 2.2. Failure envelope for the granite (Hoek and Brown criterion).

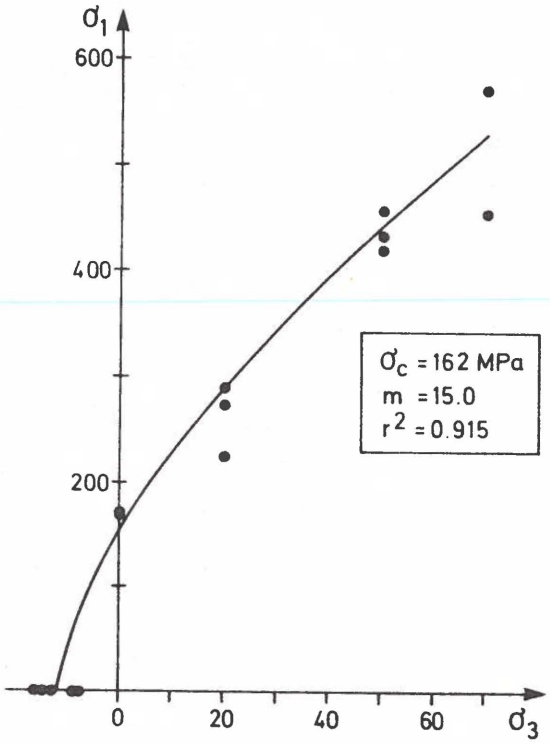


Fig.2.3. Failure envelope for the gneiss (Hoek and Brown criterion).

3 FIELD EQUIPMENT

3.1 Field instrumentation

During 1987 and 1988 a totally new hydrofracturing field unit was constructed. The entire instrumentation is installed in a new field truck. From a functional point of view the field equipment may be divided into the following components:

- Multihose, drum and guide wheel
- Borehole tools
- Water pump and control system
- Data acquisition system

The multihose is 1000 m in length, composed of 3 high-pressure hoses, 2 signal cables each containing 8 conductors and 1 kevlar stress member to carry the load of the hose. The outer diameter of the multihose is 40 mm. A cross section of the field unit and multihose is shown in Fig. 3.1. A complete description of the 1000 m hydrofracturing unit can be found in Bjarnason and Torikka (1989).

During measurements, both for hydraulic fracturing and HTPF tests, two different borehole systems are used:

- A straddle packer system. This configuration is used to initiate hydraulic fractures in a sealed-off part of the borehole during hydraulic fracturing measurements, while it is used for the reopening of preexisting fractures for HTPF tests.
- An impression packer with attached compass to identify and determine orientation and dip of initiated or natural fractures.

The straddle packer is composed of two high pressure packers (1 m in length), separated by the 65 cm long test section. The impression packer is a single packer, 2 or 3 m in length, covered by a soft impression rubber, Fig. 3.2. Both packer setups are supplied with a special pressure-release valve, to outlet the remaining pressure from the packer after depressurizing the packer line at surface. All packer elements are made of inexpensive, nylon reinforced rubber hoses, with pressed-on steel bindings. The maximum differential pressure for the packers is about 40 MPa.

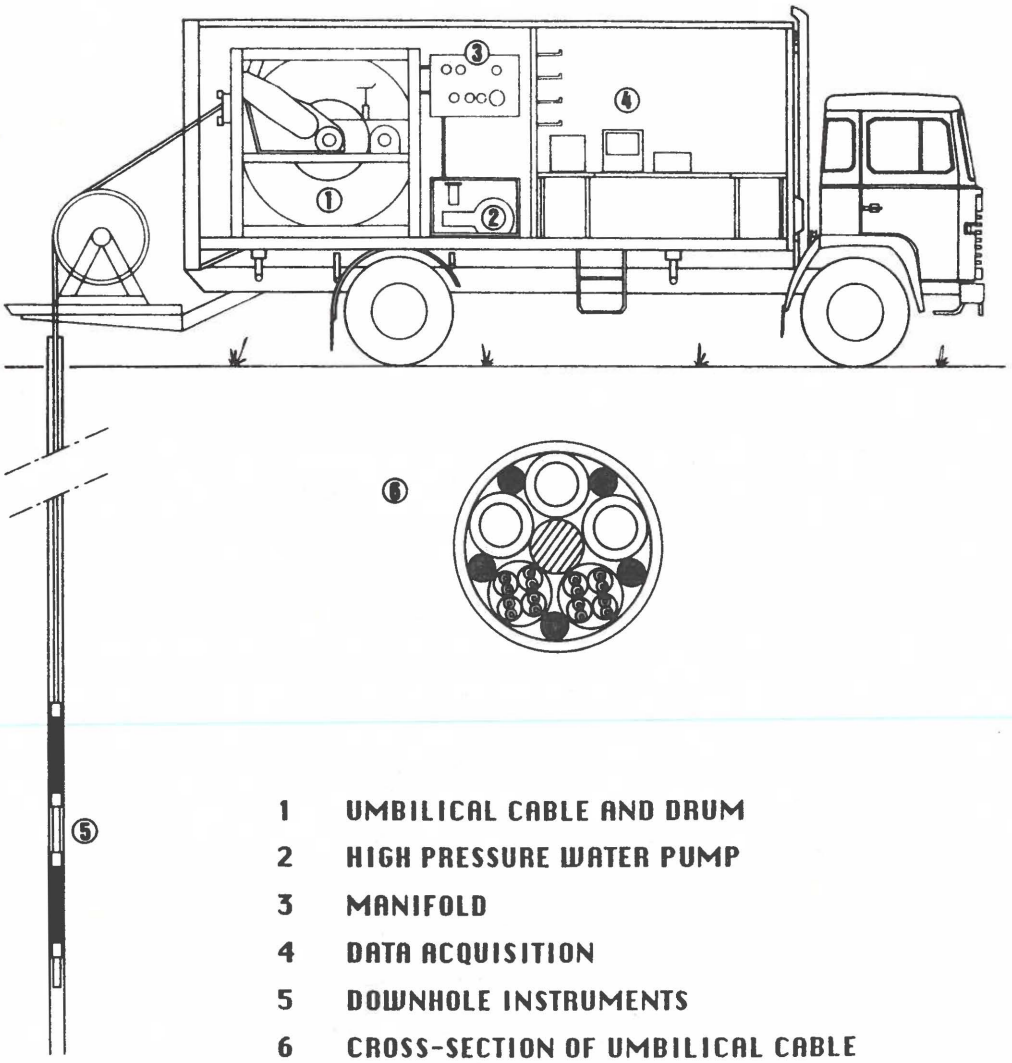


Fig 3.1. Cross section of hydrofracturing field unit and multi-hose.

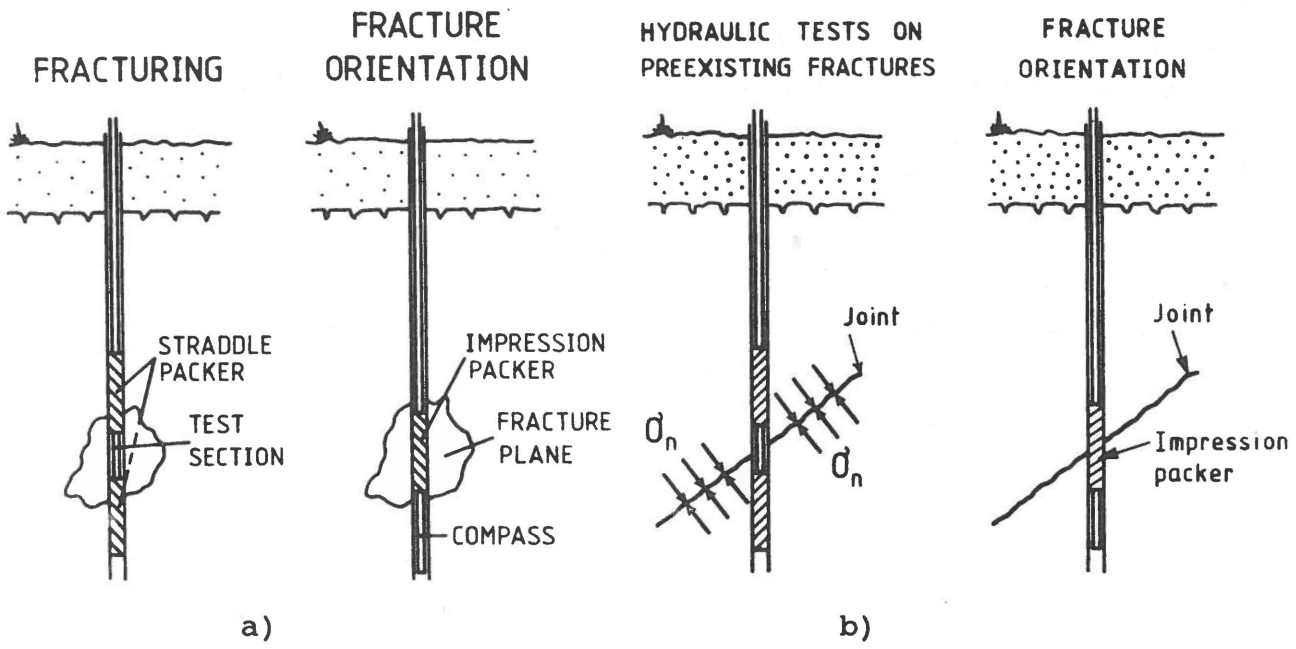


Fig. 3.2. Packer configuration in the borehole during testing. a) hydraulic fracturing, b) HTPF tests.

Water at high pressure is supplied by a hydraulically driven 3 cylinder piston pump. The maximum flow rate is 15 l/min and the maximum pressure is 100 MPa. During tests, the pressure from the pump is set to a predetermined value by a bypass valve.

The packer pressure and the test pressure are controlled independently of each other by different hoses running down the hole. This allows the packers to be pressurized parallel with the test section, avoiding high stress concentrations in the borehole wall at the ends of the straddled interval.

Packer orientation during impression is recorded by a single-shot magnetic compass attached to the lower end of the packer. The photographic film from the compass shows the inclination and azimuth of the borehole and the orientation of the packers referred to magnetic North. The compass is fixed in a non-magnetic steel barrel 3 m below the packer end.

Test results are continuously recorded on a time based strip chart recorder. Test section pressure and packer pressure are recorded by pressure gauges at the outlet of the manifold. Test section pressure is also recorded by a pressure gauge mounted just above the straddle packer. The water flow is recorded by two high pressure, bladed rotor flow meters.

3.2 Field work

Before any tests were performed, a careful length calibration of the multihose against a constant length surveying tape of steel was done. The jacket of the hose is marked every meter by the manufacturer, but as the hose is somewhat elastic these marks can not be relied upon as exact depth indicators. In the calibration procedure readings were taken every 5 m on the reference tape and the corresponding hose marking was noted.

Measurements were conducted in 33 test points in borehole LuH. 18 of these were hydrofracturing tests conducted within what was investigated to be macroscopically unfractured sections of the borehole. The other 15 test points were located to single preexisting fracture planes. Test points were selected by examination of the core log of the hole, but also by visual inspection of the drill core.

The HTPF tests were conducted on preexisting fractures (joints) with different strikes and dips. In order to effectively isolate a single fracture plane, a minimum distance of 0.5 m is required from the test fracture to the nearest fracture in the hole. The pump tests were preceded by impressions to determine the exact depth, orientation and dip of each fracture plane.

The conventional hydraulic fracturing work was conducted after the HTPF tests had been completed in order to avoid the creation of hydrofractures at sections close to natural fractures, that later should be tested by the HTPF method.

4 HYDRAULIC FRACTURING

4.1 Stress calculations

The analytical solution to evaluate the stresses from conventional hydraulic fracturing was first presented by Hubbert and Willis (1957). The solution presented by them will from here on be referred to as the classical theory. The other stress evaluation technique applied on the field results is based on a three-dimensional analysis and the Hoek and Brown failure criterion, Ljunggren (1987).

What applies to both theories is that the rock is considered as to be isotropic, linear elastic and impermeable. In the case of the LuH measurements, the principal stresses are assumed to be oriented horizontally and vertically where the vertical stress, σ_v is parallel to the axis of the borehole and equal to the overburden stress;

$$\sigma_v = \gamma z \qquad (1)$$

where γ is the unit weight of the overlying rock material and z is the vertical depth.

4.1.1 Classical theory

The calculation of stresses is based on a simple two-dimensional analytical solution of stresses around a circular opening in an infinite plate. The solution only considers stresses in a plane perpendicular to the borehole axis. Since the rock material is assumed to be isotropic, the hydrofracture will initiate in the borehole wall in a vertical plane perpendicular to the minimum horizontal stress, σ_h. The magnitude of the minimum horizontal stress is assumed to be equal to the shut-in pressure, P_s obtained when the hydraulic pressure in the fracture is in equilibrium with the stresses acting across the fracture plane, i.e.

$$P_s = \sigma_h \qquad (2)$$

The tangential stress, σ_t in the wall of the borehole at the point of fracture initiation is given by:

$$\sigma_t = 3\sigma_h - \sigma_H \qquad (3)$$

Further, the theory prescribes that to create a fracture in intact rock, both the tangential stress at the borehole wall and the tensile strength of the rock, T must be compensated by the applied hydraulic pressure. The first breakdown pressure P_{b1} at the moment of fracture initiation is thus;

$$P_{b1} = 3\sigma_h - \sigma_H + T \qquad (4)$$

from which

$$\sigma_H = 3\sigma_h + T - P_{b1} \qquad (5)$$

The hydrofracturing tensile strength in eq. (5) can be estimated from the field records or measured in the laboratory. The field tensile strength, T_f is estimated as the difference between the first and second breakdown pressures, $T_f = P_{b1} - P_{b2}$. The laboratory hydraulic fracturing tensile strength, T_{lab} is measured by miniature hydraulic fracturing tests on core samples from the field borehole. The laboratory determined tensile strength has, however, to be extraploated to apply for the large diameter borehole in the field, $T_{app} = T_{lab} \cdot C$, $C < 1$. Despite this, T_f and T_{app} tend to disagree and the choice of tensile strength for eq. (5) thus affects the calculated magnitude of the maximum horizontal stress.

The two methods of calculating σ_H, by the tensile strength obtained from laboratory tests or the field tensile strength, are referred to as the first- and second breakdown methods, respectively.

First breakdown method:

$$\sigma_{HI} = 3\sigma_h - P_{b1} + T_{app} \quad (6)$$

Second breakdown method:

$$\sigma_{HII} = 3\sigma_h - P_{b2} \quad (7)$$

4.1.2 Theory using the Hoek and Brown Failure criterion

The theoretical background of this method for calculation of in-situ stresses from hydrofracturing measurements is only summarized here. A more detailed description can be found in Ljunggren (1987). It is based on three-dimensional solution of the stresses around a circular hole in an infinite, linearly elastic and homogeneous continuum loaded at infinity Kirsch (1898).

The hole is subjected to a radial internal hydraulic pressure. In an isotropic material the tangential and vertical stresses will reach their least magnitude at points parallel to the direction of σ_H. At these points, the radial, tangential and longitudinal stress components are equal to:

$$\sigma_r = P_i \quad (8a)$$

$$\sigma_t = 3\sigma_h - \sigma_H - P_i \quad (8b)$$

$$\sigma_z = \gamma z - 2\nu(\sigma_H - \sigma_h) \quad (8c)$$

where ν is the Poisson's ratio of the rock.

Whenever the two horizontal stresses σ_H and σ_h are not equal, tensile fracturing can occur in a vertical or horizontal plane, since, from eqs.(8) σ_t or σ_z may be tensile. In the case of a vertical fracture σ_t has reached a tensile value such that a

fracture has been initiated. It can also be shown that σ_r has a larger magnitude compared to σ_z at failure, and is therfore the maximum principal stress at failure;

$$\sigma_r > \sigma_z > \sigma_t$$

By application of the Hoek and Brown failure criterion, Hoek and Brown (1980), which takes into account the maximum and minimum principal stress at failure, the maximum horizontal stress can then be evaluated. For intact rock, the criterion has the following form:

$$\sigma_1 = \sigma_3 + \sqrt{m\sigma_c\sigma_3 + \sigma_c^2} \tag{9a}$$

$$T = \frac{\sigma_c}{2}\left[\sqrt{m^2 + 4} - m\right] \tag{9b}$$

where σ_c is the unconfined compressive strength of the intact rock. m is an empirical constant that depends on the properties of the rock and on the extent to which it had been broken before being subjected to the failure stresses σ_1 and σ_3.

Since $\sigma_3 = \sigma_t$ and $\sigma_1 = \sigma_r$ in this case, we then have

$$\sigma_r = \sigma_t + \sqrt{m\sigma_c\sigma_t + \sigma_c^2} \tag{10}$$

Insertion of the expressions for σ_r and σ_t at hydraulic fracture initiation then results in:

$$P_{b1} = 3\sigma_h - \sigma_H - P_{b1} + \sqrt{m\sigma_c(3\sigma_h - \sigma_H - P_{b1}) + \sigma_c^2} \tag{11}$$

Equation (11) together with $\sigma_h = P_s$ can then be used to evaluate the maximum horizontal stress from hydrofracturing measurements that have resulted in vertical fractures.

4.2 Data analysis

4.2.1 Breakdown pressures

A typical curve from a hydrofracturing test in LuH is shown in Fig. 4.1. The first breakdown pressures have been selected visually as the pressures where the curves begin to deviate from linearity, shortly before peak pressures are reached. The second and subsequent breakdown pressures, (reopening pressures), are selected in the same way.

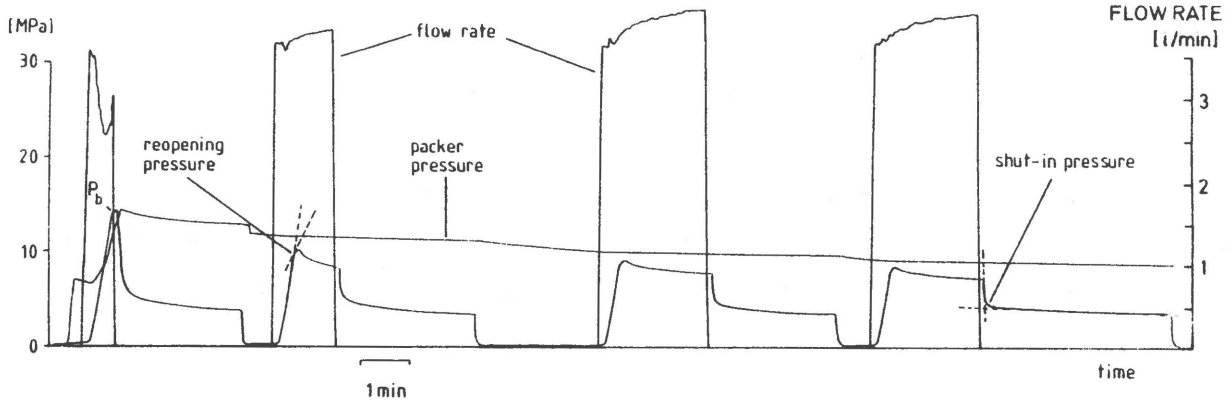


Fig. 4.1. Typical hydrofracturing field record in borehole LuH.

4.2.2 Shut-in pressures

"Shut-in" pressures (normal stresses to the fracture planes) have been measured in two different ways:

- Tangent method: The shut-in pressure is determined from an intercept of tangent lines to the pre-shut-in and post-shut-in parts of the curves, Fig. 4.1.

- Hydraulic jacking: Water is injected in steps of constant pressure, starting well below the expected shut-in pressure, stepwise increasing the pressure until the fracture is evi-

dently open. The jacking pressure, defined as the pressure at which the pressure flow relationship becomes non-linear, provides an estimate of the normal stress to the plane of the fracture, Doe (1987), Fig. 4.2. All pressure-flow diagrams from the jacking tests are presented in Appendix 2.

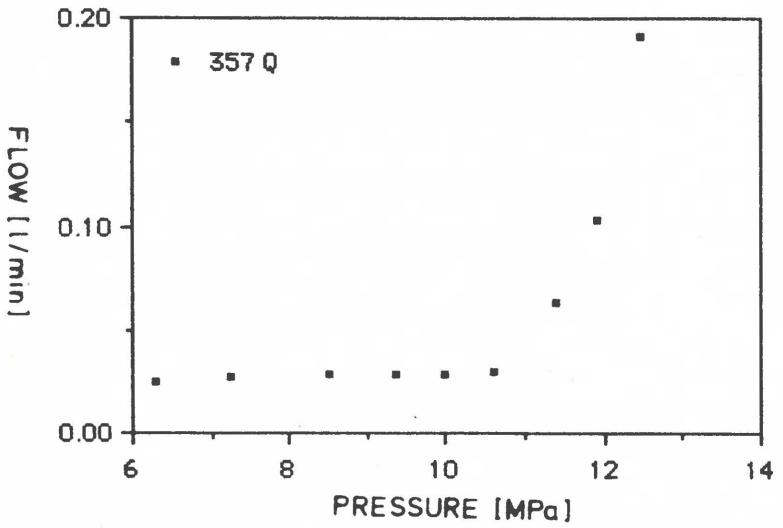


Fig. 4.2 A pressure-flow diagram to obtain the jacking pressure of a fracture, borehole LuH, depth 357.0 m.

4.2.3 Tensile strength

The hydraulic fracturing tensile strength on 20 core samples from borehole LuH was tested in the laboratory. The test setup is shown in Fig. 4.3. The core samples were taken from 6 depth intervals of the borehole, Table 4.1. The specimens were drilled through by a centered, 10 mm hole. The samples were pressurized by water, at zero confining pressure, and the pressurization rate was kept similar to that used in the field experiments. Most of the samples broke in the direction of the the foliation planes that were present in the samples. The mean laboratory tensile strength for selected depth intervals is given in Table 4.1.

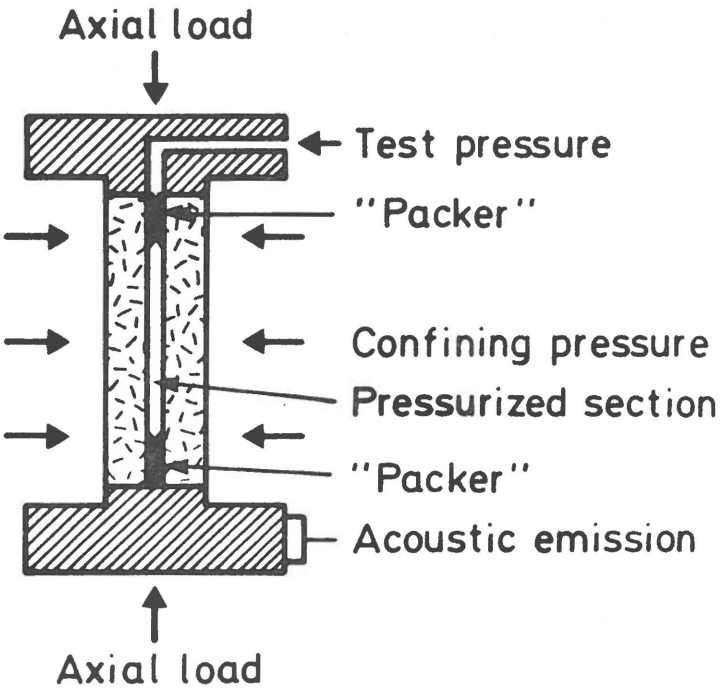


Fig. 4.3. Laboratory simulation of hydraulic fracturing for determination of the tensile strength.

Table 4.1. Measured and applied tensile strength for the rock samples from borehole LuH.

Depth (m)	Grain size (mm)	T_{lab} (10 mm) (MPa)	T_{app} (56 mm) (MPa)
50	4	6.6	3.8
80	3	11.7	7.1
180	1.5	10.7	7.2
290	3.5	13.8	8.0
370	2	12.9	8.2
460	1	16.0	11.7

How to extrapolate the small scale laboratory data to the full size borehole in the field is still uncertain. Here we apply a deterministic fracture mechanics approach, based on Paris and Sih (1965) and used by Doe et al. (1983). With largest grain sizes given i Table 4.1, laboratory borehole of 10 mm in diameter and a field borehole of 76 mm we obtain the applied tensile strength values, T_{app} for the calculation of σ_H shown in Table 4.1.

4.3 Results and interpretation

Totally, hydrofracturing measurements were conducted at 18 points, evenly distributed between 46 m depth down to 494 m depth. Out of these, 8 resulted in single or subhorizontal hydrofractures. The results from the hydrofracturing measurements are therfore only based on the remaining 10 successfully completed test points.

The compiled pressure data from the 10 successfully completed tests are shown in Table A1, Appendix 1. Calculated rock stresses are presented in Tables 4.2 and 4.3 in this chapter. The minimum horizontal stress was calculated according to the tangent method described in section 4.2.2. The pressure data from the hydraulic jacking tests are shown in Appendix 2. The results from the oriented fracture impressions are presented in Table A2, Appendix 1.

As is shown in Table 4.3, two columns of maximum horizontal stress magnitudes are presented. The σ^B_{HI} magnitudes were evaluated by application of the m values obtained from the laboratory tests, cf. Figs. 2.2 and 2.3. The σ^B_{HII} magnitudes were calculated using T_{app}, Table 4.1, to obtain the value of the empirical constant m, (eqs. (9a) and (9b)). For both evaluation procedures, the empirical constant s in the failure criteria was set equal to 1.

Table 4.2. Calculated rock stresses from hydraulic fracturing measurements in borehole LuH. The maximum horizontal stress is evaluated according to the classical theory.

					First break-down method		Second break down method	
	Field tens str.	Appl tens str.	Vertical str.	Min. horiz. str.	Max. horiz. str.	Horiz str. ratio	Max. horiz. str.	Horiz str. ratio
Depth (m)	T_f (MPa)	T_{app} (MPa)	σ_v (MPa)	σ_h (MPa)	σ^c_{HI} (MPa)	$\frac{\sigma^c_{HI}}{\sigma_h}$	σ^c_{HII} (MPa)	$\frac{\sigma^c_{HII}}{\sigma_h}$
46.0	3.75	3.8	1.2	3.6	5.0	1.4	5.0	1.4
98.6	3.9	7.1	2.6	4.8	8.5	1.8	5.3	1.1
138.3	5.7	7.1	3.6	7.2	12.4	1.7	11.0	1.6
221.4	4.0	7.2	5.8	9.4	21.6	2.3	18.4	2.0
248.6	6.3	7.2	6.5	8.7	15.2	1.7	14.3	1.6
304.8	10.5	8.0	7.9	9.0	13.2	1.5	15.7	1.7
323.3	9.9	8.0	8.4	9.1	12.3	1.4	14.2	1.6
357.0	3.0	8.2	9.3	11.4	23.8	2.1	18.6	1.6
477.8	7.2	11.7	12.4	14.0	29.7	2.1	25.2	1.8
494.2	4.8	11.7	12.8	13.9	28.8	2.1	21.9	1.6

Table 4.3. Calculated rock stresses from hydraulic fracturing measurements in borehole LuH. The maximum horizontal stress is evaluated according to the theory using the Hoek and Brown failure criterion.

					Determ. by using m_{lab}		Determ. by using $m_{T(app)}$	
			Vertical str.	Min. horiz. str.	Max. horiz. str.	Horiz str. ratio	Max. horiz. str.	Horiz str. ratio
Depth (m)	m_{lab}	$m_{T_{app}}$	σ_v (MPa)	σ_h (MPa)	σ^B_{HI} (MPa)	$\frac{\sigma^B_{HI}}{\sigma_h}$	σ^B_{HII} (MPa)	$\frac{\sigma^B_{HII}}{\sigma_h}$
46.0	15.0	42.6	1.2	3.6	11.9	3.3	5.0	1.4
98.6	17.6	36.6	2.6	4.8	16.0	3.3	8.5	1.8
138.3	15.0	22.8	3.6	7.2	15.8	2.2	12.4	1.7
221.4	15.0	22.4	5.8	9.4	25.0	2.7	21.5	2.3
248.6	15.0	22.4	6.5	8.7	18.5	2.1	15.0	1.7
304.8	17.6	32.5	7.9	9.0	19.7	2.2	13.1	1.5
323.3	15.0	20.2	8.4	9.1	14.7	1.6	12.0	1.3
357.0	15.0	19.7	9.3	11.4	26.1	2.3	23.6	2.1
477.8	17.6	22.2	12.4	14.0	32.5	2.3	29.5	2.1
494.2	17.6	22.2	12.8	13.9	31.6	2.3	28.6	2.1

4.3.1 Stress magnitudes

The minimum horizontal stress, σ_h is around 4 MPa at 50 m depth. Down to 500 m depth it increases steadily at a rate somewhat less than that of the vertical stress, σ_v, Fig. 4.4. The results shows that σ_h is the intermediate principal stress down to 500 m depth. As the stress difference between the magnitudes of σ_h and σ_v is small in the deeper regions the stress state can be described as close to isotropic between 400 - 500 m in the vertical plane containing $\sigma_h$and σ_v.

Compared to other stress measurements in Sweden, (Bjarnason and Stephansson (1986), Stephansson annd Ångman (1986) and Bjarnason (1986)), the minimum horizontal stress shows about the same gradient and magnitudes.

For the maximum horizontal stress the situation is more complicated:

The evaluation based on the classical theory and the first breakdown method results in a larger scatter of the maximum horizontal stress compared to what is obtained by the second breakdown method, cf Fig. 4.4. The scatter is most pronounced between 200 m and 300 m depth. As an example we get 21.6 MPa at 221.4 m depth and 13.1 MPa at 304.8 m depth. The ratio between σ^{C}_{HI} and σ_h is plotted as a function of depth in Fig.4.5. The ratio is fairly stable with depth having a value just below 2.

The magnitudes of maximum horizontal stress determined by application of the second breakdown method, σ^{C}_{HII} are somewhat lower than σ^{C}_{HI}. The scatter, however, is found also in these results although it is not that pronounced. The ratio of $\sigma^{C}_{HII}/\sigma_h$ is stable through the entire measuring depth, Fig. 4.5, having a nearly constant value around 1.6.

The magnitudes of the maximum horizontal stress, evaluated by application of the Hoek and Brown criterion, is presented as function of depth in Fig.4.6. Two different approaches of evaluation is presented as discussed before in this chapter. The σ^{B}_{HI} results are evaluated by use of the m and s values (s = 1) determined from the laboratory tests, and as can be seen this results in higher values through the entire measuring depth compared to σ^{B}_{HII}, determined by application of T_{app} to get the m value. The ratio σ^{B}_{HI}/σ_h, Fig. 4.5, results in values above 3 for the most superficial test points wheras the remaining ratios are fairly stable around 2.2. For $\sigma^{B}_{HII}/\sigma_h$ we have a nearly constant ratio as function of depth.

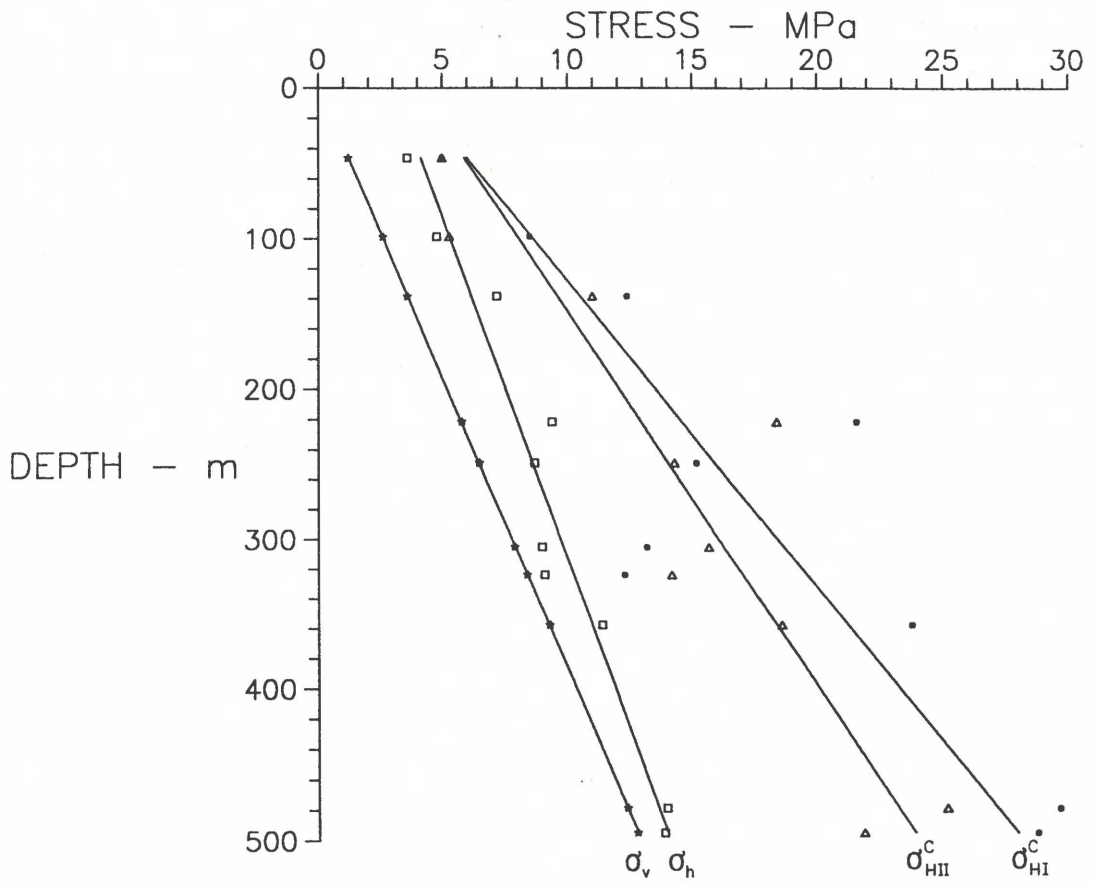


Fig. 4.4. Calculated rock stresses as a function of depth in borehole LuH. The calculations have been done according to the classical theory.

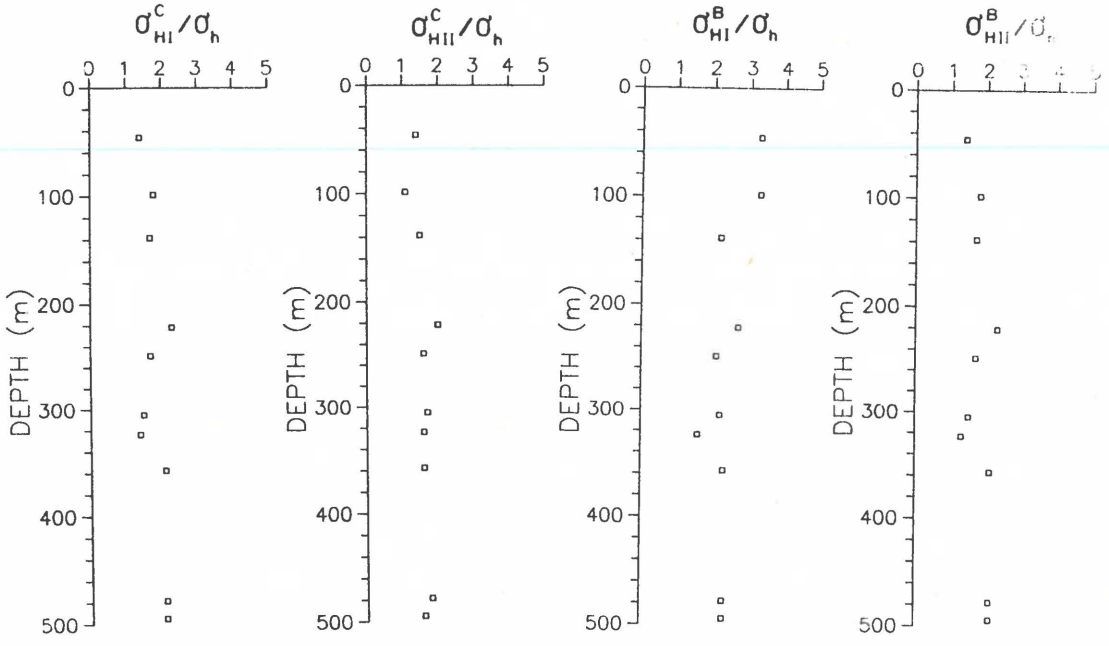


Fig. 4.5. The ratio of maximum to minimum horizontal stress.

In Figs. 4.4 and 4.6 the stresses have also been treated by linear regression analyis. The points for the minimum horizontal stress are all close to the fitted line, whereas the maximum horizontal stress show a large scatter around the best fit line. All four sets of σ_H-magnitudes show the same picture; A rather large magnitude increase down to 220 m depth, then a rapid decrease in the interval 220 m - 320 m, and then an increase of the magnitude down to 500 m depth.

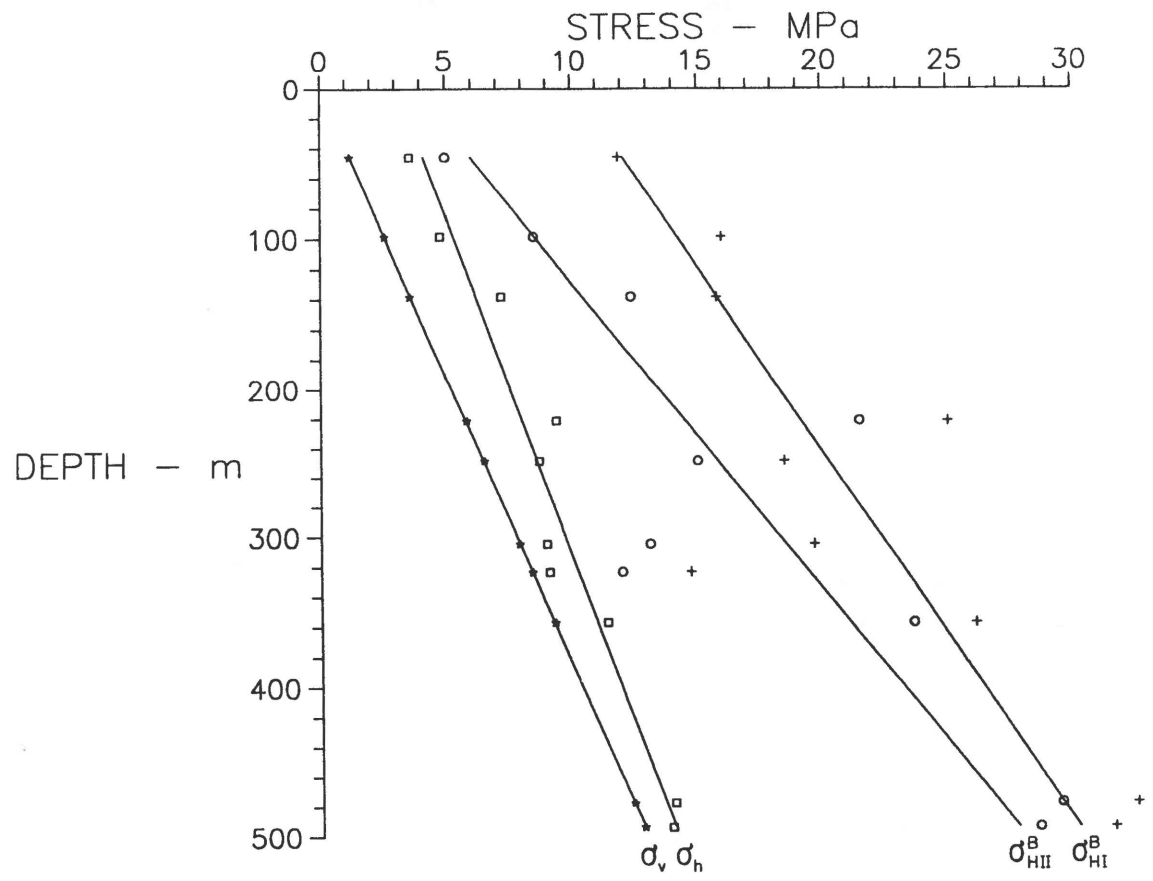


Fig. 4.6. Calculated rock stresses as a function of depth in borehole LuH. The calculations have been done by use of the Hoek and Brown failure criteria.

4.3.2 Stress orientations

Two long and vertical hydrofractures were observed at 7 test sections. The direction of the maximum horizontal stress at each test section is taken as the mean strike of the two fractures at the corresponding depth. All exept one fracture fall within a sector of approximately 30 degrees, striking from N17°W to N14°E., Fig. 4.7. The outlier is noted at 477.8 m depth. If this point is excluded in the evaluation, we obtain a mean strike for the remaining 6 points of N-S. This value is taken to represent the average orientation of the maximum horizontal stress determined by hydraulic fracturing. The standard deviation of the mean strike is 12°.

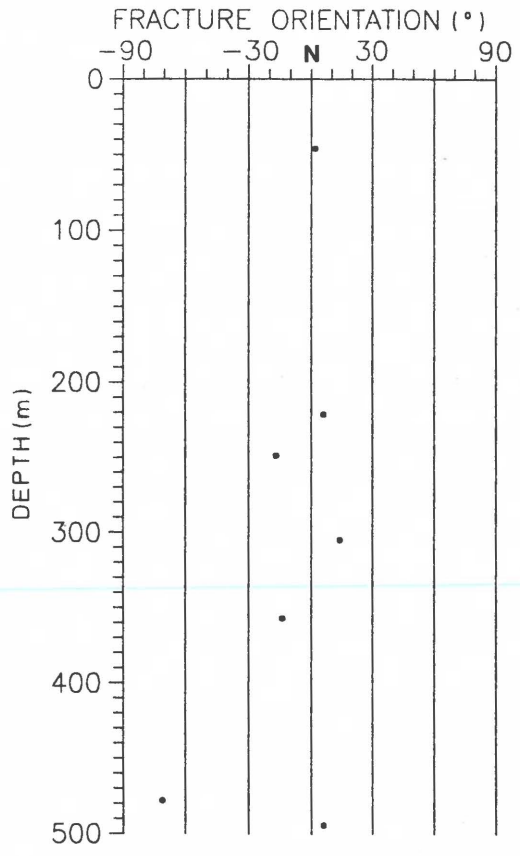


Fig. 4.7. Hydrofracture orientations in borehole LuH at luleå.

4.3.3 Interpretation

We begin with the obtained orientation of the stress field, since the direction of induced fractures indeed influence the calculated stress magnitudes. We then recall that the obtained orientation of σ_H is based on only 6 fracture directions of the 18 oriented impressions that were done, which can not be considered as a satisfied result. Several impressions on induced fractures, excluded in the evaluation, clearly showed how the fractures lined up with the subvertical planes of the foliation. Röshoff and Norin (1981) investigated cores from the boreholes in the rock heat store a few hundred metres from the LuH borehole and found pronounced steep planes of foliation oriented N-S. This was also found by Ludwig (1981) by mapping on outcrops in the same area. As can be seen in Appendix 3, 14 of 17 laboratory hydraulic fracturing tests on gneissic core specimens resulted in fractures induced along the foliation planes.

Based on the evidence that N-S striking, steep foliation planes exist in the gneiss, two sleeve fracturing tests were decided to be done. By sleeve fracturing is meant pressurization by a packer until fracturing of the rock occurs. In such a test no fluid is introduced into the rock during the fracturing process. One then avoids the introduction of stress concentrations at micro fractures and planes of weakness in the borehole wall. In this study we used a 2 m long packer element to fracture the rock. Two fracture free sections, at 237.4 m and 444.0 m, were selected. Both tests gave two, 2 m long vertical fractures and the obtained fracture directions were N41°W and N43°W, respectively.

The approximately N40°W direction for the maximum horizontal stress obtained from the sleeve fracturing tests are not found for any of the hydraulic fracturing induced fractures, Fig. 4.7. It seems therefore that the hydrofracturing induced fractures have been affected by the steep weakness planes, striking N-S, that are present in the rock.

The maximum horizontal stress magnitudes have been evaluated in 4 different ways. The classical method of evaluation assumes that a hydraulic fracture is initiated when the stress concentration, $3\sigma_h - \sigma_H$ at the borehole wall, and the tensile strength of the rock are exceeded. The failure criteria of the classical analysis says that the tangential stress, σ_t is equal to -T at failure. Figure 4.8 below shows that the above failure criteria is only valid for the case when $\sigma_1 = 0$, ($\sigma_1 = \sigma_r$). This case, however, never occurs in hydraulic fracturing, since the pressure, P required to initiate a fracture is always greater than zero, ($\sigma_1 = \sigma_r = P$). How much this affect the calculated rock stresses depends on the shape and path of the failure envelope for the rock type. For most rocks, including the rock in the LuH borehole, the above assumption can be considered as applicable.

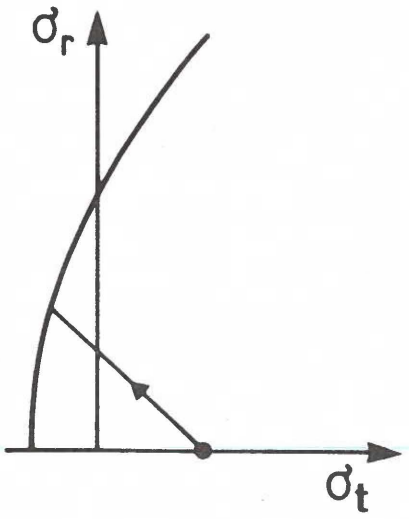


Fig. 4.8. Failure envelope and stress path for hydraulic fracturing tests when axial fractures are initiated.

Applying the first breakdown method we assume that it is correct to extraploate laboratory tensile strength data to the 56 mm hole in the field. Furthermore we assume a uniform tensile strength within depth intervals given in Table 4.2. The first assumption is difficult to verify. For the second assumption we

recall the results from the laboratory hydraulic fracturing tests on drillcores from LuH, Table 4.1 and Appendix 3. Each figure in the table is a mean value from a series of tests, and the variation for individual specimens within each depth interval is not neglectable. The assumption of uniform tensile strength is therefore not ideal.

The use of the second breakdown method rests on the assumption that no water penetrates the hydrofracture during pressurization in the second and subsequent cycles. Accordingly the fracture is assumed to open up suddenly when the borehole pressure reaches the value of $3\sigma_h - \sigma_H$. For a constant pumping rate in all cycles the pressure build-up and reopening curve should be a replica of the first pressurization cycle, up to the point of reopening. Figure 4.1, which is a typical field record from the hydrofracturing tests in LuH, shows that the curves from these measurements satisfy the above assumption.

The evaluation using the Hoek and Brown criterion has the advantage of taking into account the influence of the vertical and radial stresses at the borehole wall, Ljunggren (1987). The problem with applying this technique, however, is to get relevant data of the empirical constants m and s in the failure criteria, that applies to the field conditions. Two approaches were used in this study. In one, the m value determined from the failure envelopes of intact rock strength on core samples was used. The assumption in this approach is that small scale laboratory strength is directly applicable to field data. Even if the sealed-off section in a hydrofracturing test is totally free from macroscopic fractures we know by experience that its strength is less compared to laboratory strength. Thus, the approach of adopting the empirical constant m from laboratory tests is obviously not a good one.

The second evaluation approach, using the Hoek and Brown criteria, is in one aspect similar to the first breakdown method. We adopt the tensile strength, T_{app} in Table 4.1 to back calculate the m value, (eq. (9b)). As a result thereof, the maximum

horizontal stress obtains similar magnitudes as σ_{HI}^{c}. Again, the extrapolation of T_{lab} to T_{app} is difficult to verify, plus that that the assumption of a uniform tensile strength within depth intervals is not ideal.

Based on the above discussion the authors adopt the second breakdown method to determine the maximum horizontal stress at Luleå.

The validity of linear regression analyses made on the σ_H-data in Figs. 4.4 and 4.6 may be questioned since the data are so scattered. The reason, however, for showing the regression lines is to give a picture of the σ_H-trend as function of depth. The fracture zone between 150 - 170 m depth do not show any influence on the stress magnitudes, wheras the the maximum horizontal stress show a negative gradient as approaching the fracture zone between 346 - 350 m depth. It is not belived, however, that this negative gradient is caused by the existence of the fracture zone, and the argument for that is that the rock in the section logged as fracture zone only show heavily fracturing for about 2 metres when inspecting the core. The negative gradient can instead be explained by the high σ_H-magnitude obtained at 221.4 m depth. If this data point is excluded in the graph, the scatter would not be large. As can be seen in Fig. 4.4 the σ_h-magnitude at depth 221.4 m is approximately 1.5 MPa larger compared to what is obtained from the fitted line at this depth. As a consequence of the equation for stress evaluation, this increase for σ_h is threefolded for σ_H.

5 HYDRAULIC TESTS ON PREEXISTING FRACTURES

5.1 Introduction

The technique of hydraulically pressurize preexisting fractures intersecting the borehole wall to determine the stress state was first presented by Cornet (1981) and Cornet and Valette (1984). It has so far been used at three sites in Sweden; Gideå, Stripa and the LuH tests. The method is based on the measurement of the normal stress acting across fracture planes with different strikes and dips. Compared to hydraulic fracturing this method has the advantage of, in favourable situations, provide means for the determination of the three-dimensional stress field.

5.2 Theory

The idea of developing an alternative method to determine the stress state in deep boreholes partly came to live because of situations where hydraulic fracturing is inapplicable. Such situations are:

- Test in vertical boreholes where the principal stresses are not horizontally and vertically oriented.

- When the test borehole is inclined to the vertical and the principal stresses are oriented in the vertical and horizontal plane.

If a test section is intersected by a preexisting fracture plane the assumptions of the hydrofracturing method do not strictly apply. When pumping is conducted in such a section, the existing fracture plane may open up and propagate along the existing plane as the pumping continues. This is, however, not always the case and axial hydrofractures can, under certain circumstances be initiated crossing natural fractures. Factors controlling the initiation of axial hydrofractures within naturally fractured

sections are; i) the in-situ stress field, ii) the degree and type of healing of the natural fractures, and iii) the pressurization rate applied and the viscosity of the fracturing fluid.

To ensure the reopening of a natural fracture without creating hydrofractures the pressurization rate must be kept low enough to allow fluid to build up in the fracture before opening. Otherwise an axial hydrofracture may be initiated and the information on the normal stress sought from the natural fracture plane will be lost.

The interpretation of HTPF pressure - time curves are identical to the interpretation of conventional hydrofracturing tests:

- A "breakdown" pressure is recorded. However, for a HTPF test this value has no physical significance and is not used in any part of the evaluation.

- A shut-in pressure is recorded. This corresponds to equilibrium between the hydraulic pressure in the fracture and the fracture normal stress.

For a test on a natural joint plane the shut-in pressure, P_s is equal to:

$$P_s = \sigma_n \tag{12}$$

where σ_n = normal stress acting across the joint plane.

A successful HTPF test will give give information on; i) shut-in pressure on the fracture plane, ii) strike and dip of the fracture plane referred to a fixed global coordinate system, and iii) the depth of the test point.

For a test we have the following relation:

$$\vec{\sigma n} \cdot \vec{n} = \sigma_n \tag{13}$$

where
$\bar{\sigma}$ = stress tensor at the test location
$\vec{n}$ = unit normal to the fracture plane

5.3 Modelling of the stress state

The stress tensor $\bar{\sigma}$ involves 6 functions of the 3 components of the unit normal vector $\vec{n}$. The solution of eq. (13) therefore depends on the assumptions made for the mathematical expression of the 6 functions so that the number of unknowns may be reduced. The number of tests required for the complete determination of the stress tensor depends on the assumptions made and several alternatives are possible, cf. Ljunggren and Raillard (1987). The two models used in this work are presented below.

5.3.1 Three-dimensional model

In this three-dimensional case tests are performed at different depths and the model provides a three-dimensional calculation of the stress tensor with depth. To solve the inverse problem expressed in eq. (13), no lateral variation of σ is permitted. This assumption is valid when the tests are conducted in a vertical or subvertical borehole. The variation of the stress tensor $\bar{\sigma}$ with depth z may then be expressed in the form:

$$\bar{\sigma} = \bar{\sigma}(z) \tag{14}$$

If the stress field is assumed to be a linear function of depth, eq. (14) gives:

$$\bar{\sigma}(z) = \bar{S} + z\bar{\alpha} \tag{15}$$

where $\bar{S}$ and $\bar{\alpha}$ are second order symmetric tensors.

In the frame Λ, see Fig. 5.1, x and y are the horizontal direc-

tions, oriented to the north and east, respectively, and z is vertical and oriented downwards. By substitution of eqs. (14) and (15) into eq. (13) we get:

$$(\bar{S} + z\bar{\alpha})\vec{n} \cdot \vec{n} = P_s \qquad (16)$$

Eq. (16) involves 12 unknowns and due to uncertainties in the measurements at least 14-15 succesful tests are required for the solution of the equation if no further assumptions are introduced.

5.3.2 Two-dimensional model

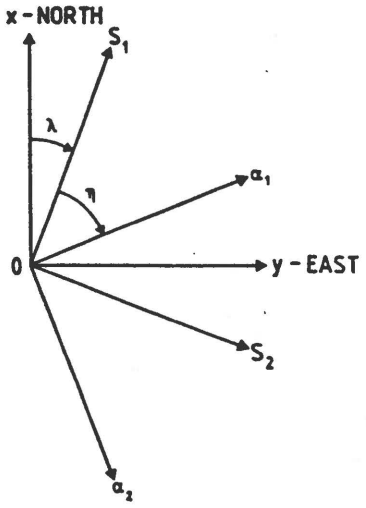
In cases when the number of successful tests available is less than what is required for a three-dimensional solution further assumptions have to be introduced and the problem then becomes two-dimensional. The stresses are assumed to have no lateral variation and to vary linearly with depth. Suppose the vertical stress is a principal stress. Then, referred to the reference frame Λ, the tensors $\bar{S}$ and $\bar{\alpha}$ take the form:

$$\bar{S} = \begin{bmatrix} S_{11} & S_{12} & 0 \\ S_{12} & S_{22} & 0 \\ 0 & 0 & 0 \end{bmatrix} \quad \text{and} \quad \bar{\alpha} = \begin{bmatrix} \alpha_{11} & \alpha_{12} & 0 \\ \alpha_{12} & \alpha_{22} & 0 \\ 0 & 0 & \alpha_{33} \end{bmatrix}$$

The number of unknowns is now 7 and may be reduced to 6 if α_{33} is assumed to be equal to the weight of the overlying rock material, γ. In the case of the LuH measurements γ was set equal to 0.026 MPa/m, and the stress component in the vertical direction is then written as:

$$\sigma_{33} = 0.026 \cdot z \qquad \text{MPa} \qquad (17)$$

The model summarized here defines the fracture by the 3 components of its unit normal vector with respect to the reference frame Λ = (north, east, depth), Figs. 5.1 and 5.2.



Λ = (North,East)

Σ = (S_1, S_2)

Ω = (α_1, α_2)

λ = angle (North, S_1)

η = angle (S_1 , α_1)

Fig.5.1. Definition of frames and angles.

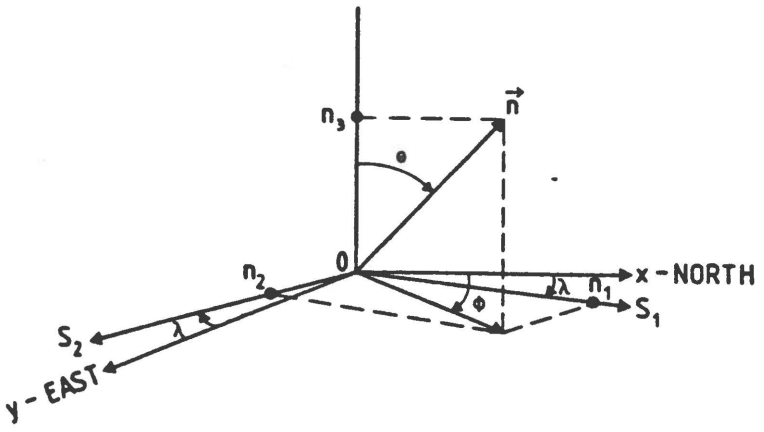


Fig. 5.2. Unit normal to the fracure plane.

Considering the experimental uncertainties of the measurements in a borehole, 8-9 tests will provide sufficient data to determine the two-dimensional stress state.

5.4 Results

Hydraulic tests were conducted on 15 joints from depths of 42.8 m down to 464.9 m. Of these, 12 were interpreted as giving reliable shut-in pressures and orientations. To facilitate a

three-dimensional stress determination, which requires 14-15 successful tests, 4 tests were selected from the hydrofracturing tests in the same borehole. These 4 tests were all reopening of joints in the borehole wall, i.e. non-successful hydrofracturing tests.

In Table 5.1 all the test points are shown together with the interpreted field results. The principal stresses in the plane perpendicular to the borehole axis are presented in section 5.4.1, and the three-dimensional stress state is presented in section 5.4.2.

Table 5.1. Test points and corresponding field results. Dip: angle between the normal to the fracture plane and vertical axis. Strike: orientation of the horizontal projection of the normal with respect to north. σ_n: normal stress supported by the fracture plane.

Depth (m)	Strike (°)	Dip (°)	σ_n (MPa)
42.8	219	81	4.35
51.0	5	42	3.95
72.4	105	27	3.6
81.3	172	13	3.55
92.1	40	25	2.1
100.9	66	72	5.2
130.9	213	23	6.15
175.6	147	80	8.25
189.0	336	33	7.65
206.4	129	62	13.3
238.8	182	37	8.75
239.5	225	81	10.55
309.1	200	82	10.5
356.2	324	8	10.2
372.1	211	59	11.1
430.8	224	71	11.2

The pole point of each fracture used in the analyses are shown in Fig 5.3. It can be seen that the strikes and dips are evenly distributed and no preferred orientation of the tested fractures are found.

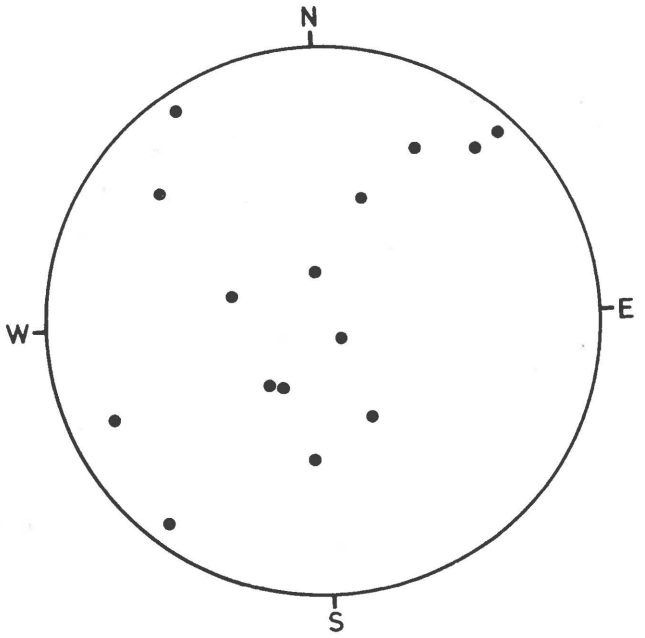


Fig. 5.3. Pole points of the preexisting fractures used for stress evaluation with HTPF.

5.4.1 Two-dimensional state of stress

The input data for the two-dimensional study are shown in Table 5.2. The test points are evenly distributed between 42.8 m and 430.8 m depth.

The standard deviation on obtained field pressure data, presented as the ε_σ parameter in Table 5.2, has been estimated from the uncertainties in interperting the field records and the quality of the pressure gauge. Similarly, the standard deviations on strike and dip have been estimated from the uncertainties in interpreting the compass and impressions. The standard deviation on depth has been estimated to be in the range of 0.1 m due to several depth calibrations against unique fracture patterns at the borehole wall.

Table 5.2. Input data for the two-dimensional stress analysis with HTPF.

Depth, z (m)		Fracture strike, Φ (°)		Fracture dip, θ (°)		Normal stress, σ_n (MPa)	
z	ε_z	Φ	ε_Φ	θ	ε_θ	σ_n	ε_σ
42.8	0.1	219	7	81	3	4.35	0.1
72.4	0.2	105	7	27	3	3.6	0.1
81.3	0.2	172	7	13	3	3.55	0.1
100.9	0.1	66	7	72	3	5.2	0.1
175.6	0.2	147	7	80	3	8.25	0.1
189.0	0.1	336	7	33	3	7.65	0.1
206.4	0.1	129	7	62	3	13.3	0.1
238.8	0.1	182	7	37	3	8.75	0.2
309.1	0.1	200	7	82	3	10.5	0.2
356.2	0.1	324	7	8	3	10.2	0.1
430.8	0.1	224	7	71	3	11.2	0.1

The magnitude of the horizontal stresses are presented in Table 5.3 and Fig. 5.4. From Fig.5.4 it can be seen that the theoretical vertical stress, ρgz is the least principal stress down to approximately 400 m. Below that and down to 430 m the stress state can be described as isotropic in the plane containing σ_v and σ_h. The maximum horizontal stress, σ_H show a rather large increase with depth resulting in 24.5 MPa at 430 m depth.

The orientation of the stresses are constant throughout the investigated depth interval, Fig. 5.5, where the orientation of the maximum horizontal stress is N37°W (143°).

Table 5.3. Calculated horizontal rock stresses with HTPF, LuH.

Depth (m)	Maximum horizontal stress σ_H (MPa)	Minimum horizontal stress σ_h (MPa)
50	6.3	4.5
100	8.7	5.4
150	11.1	6.3
200	13.5	7.3
250	15.9	8.2
300	18.3	9.1
350	20.7	10.0
400	23.1	10.9
430	24.5	11.4

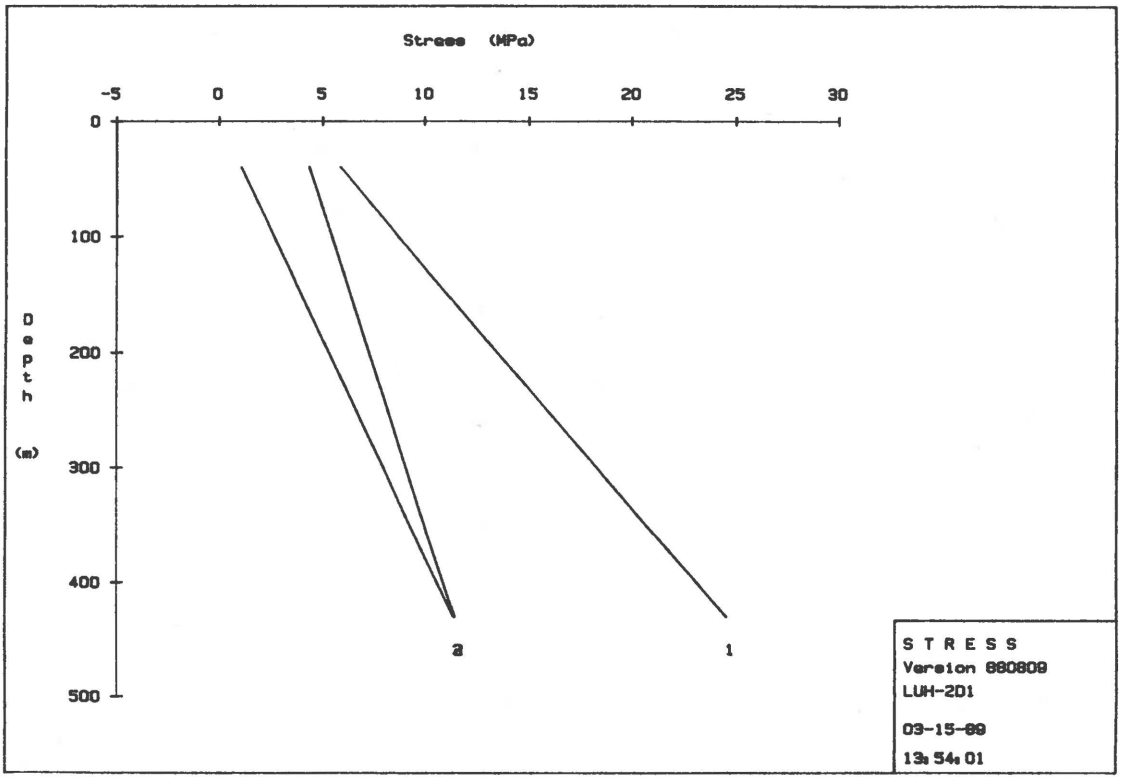


Fig.5.4. Vertical and horizontal stresses as function of depth as obtained from the two-dimensional HTPF analysis.

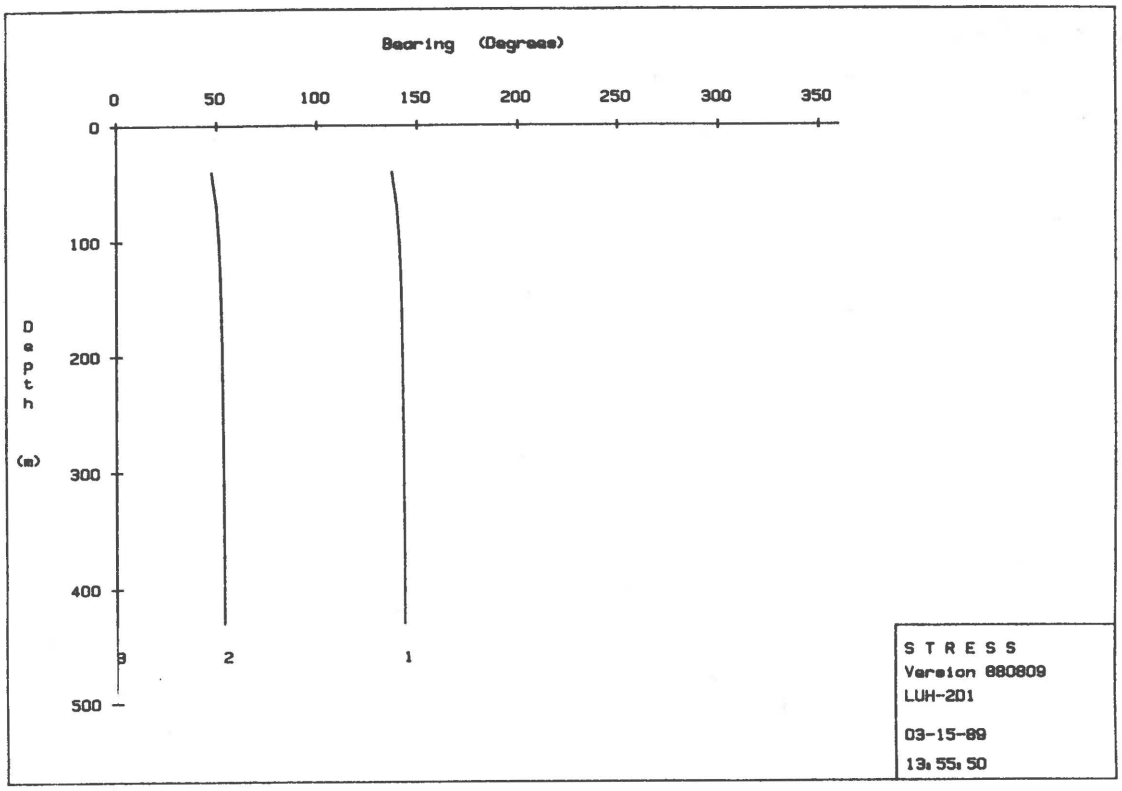


Fig.5.5. Orientation of the horizontal stresses at Luleå. Two-dimensional HTPF analysis.

If any of the data points that were included in the calculation to obtain the above presented results is subtracted from the analysis, this does not affect the results significantly. At most, the orientation changes ± 5° and the magnitudes ± 1 MPa. Thus, the solution presented can be considered as being stable.

Another technique to the verify the solution obtained, is to use the 10 uppermost data points in Table 5.1, and conduct an analysis with these data. Then move one data point down so that the total number of data points are still 10, and then perform a new analysis. Applying this technique down to the deepest measuring point allows for testing the influence of each data point on the results, and if the stress magnitudes show a non-linear behaviour and/or if the directions of the stresses change with depth. The conclusions that can be drawn from this analysis is that the orientation of the stresses is unaffected, whereas the magni-

tudes show a small gradient change for the deepest analyses. The conclusion that can be drawn, however, is that the stress magnitudes presented in Table 5.3 and Fig.5.4 are representative for the depth interval 42.8 m - 430.8 m.

5.4.2 Three-dimensional state of stress

The three-dimensional stress analysis was conducted by use of the data in Table 5.4. The standard deviations on strike and dip were set to 7° and 3°, respectively and to 0.1 MPa on the normal stress except for the data points at 238.75 m and 309.1 m where 0.2 MPa was used. The standard deviation on depth was 0.1 m except for data points 72.4 m, 81.3 m and 372.1 m where it was set to 0.2 m.

Table 5.4. Input data for the three-dimensional stress analysis.

Depth, z (m)		Fracture strike, Φ (°)		Fracture dip, θ (°)		Normal stress, σ_n (MPa)	
z	ε_z	Φ	ε_Φ	θ	ε_θ	σ_n	ε_σ
42.8	0.1	219	7	81	3	4.35	0.1
51.0	0.1	5	7	42	3	3.95	0.1
72.4	0.2	105	7	27	3	3.6	0.1
81.3	0.2	172	7	13	3	3.55	0.1
92.1	0.1	40	7	25	3	2.1	0.1
100.9	0.1	66	7	72	3	5.2	0.1
175.6	0.2	147	7	80	3	8.25	0.1
189.0	0.1	336	7	33	3	7.65	0.1
206.4	0.1	129	7	62	3	13.3	0.1
238.8	0.1	182	7	37	3	8.75	0.2
309.1	0.1	200	7	82	3	10.5	0.2
356.2	0.1	324	7	8	3	10.2	0.1
372.1	0.1	211	7	59	3	11.1	0.1
430.8	0.1	224	7	71	3	11.2	0.1

The three-dimensional calculataion showed in this case to be very sensitive to which input data that were used. The magnitudes and the directions of the principal stresses varies significantly depending on which data points the calculation is based on. The dips of the stresses are relatively unaffected. The results in Figs. 5.6 and 5.7 should therfore, because of this sensitivity, only be treated as values representing the average three-dimensional solution.

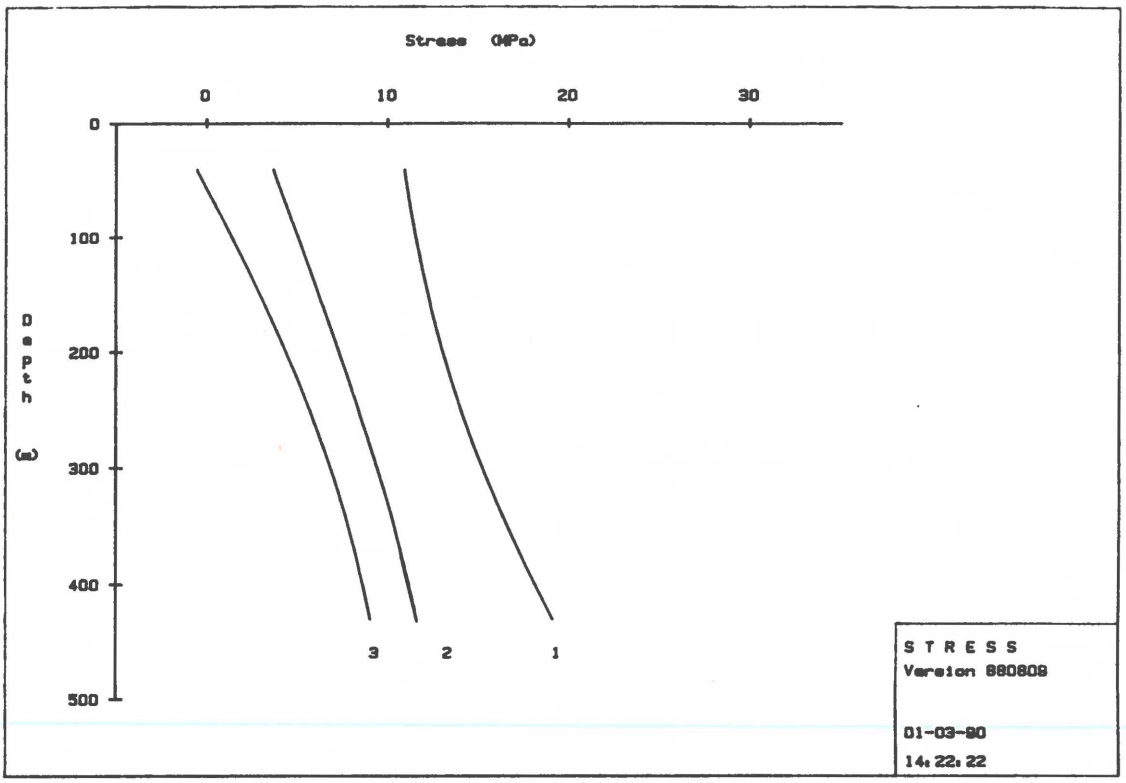


Fig. 5.6. Stress magnitudes obtained by a three-dimensional HTPF calculation.

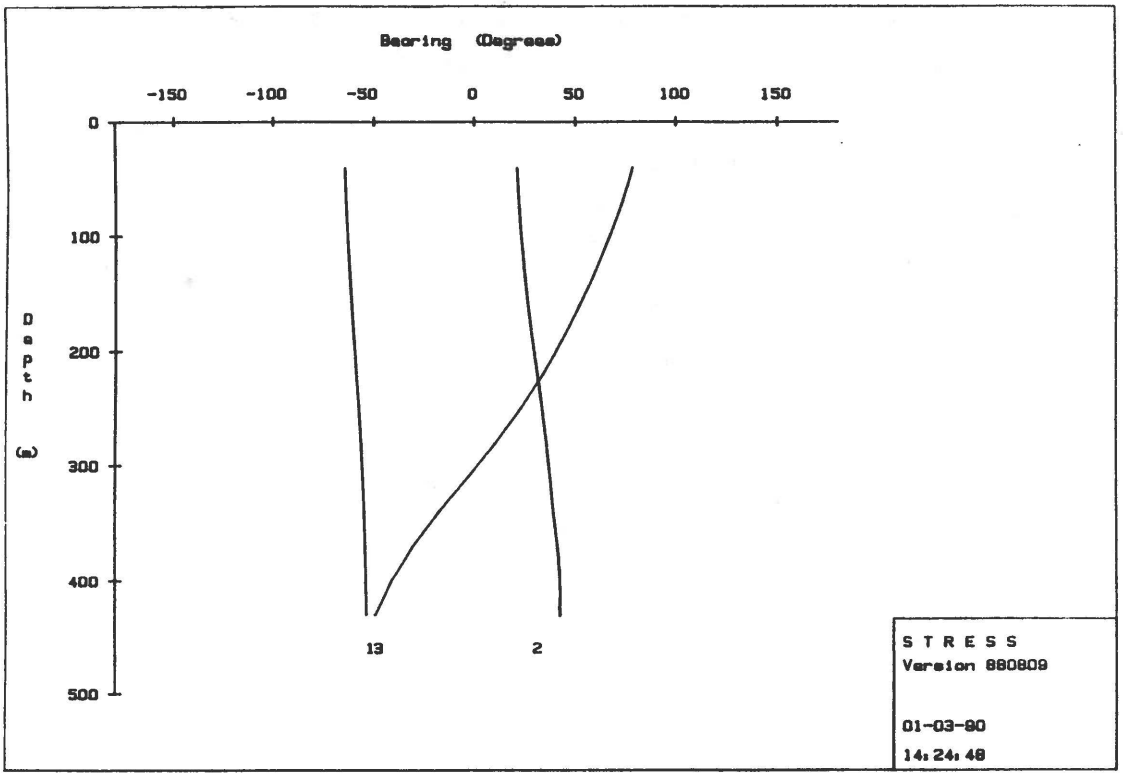


Fig.5.7. Direction of the principal stresses (3-D analysis).

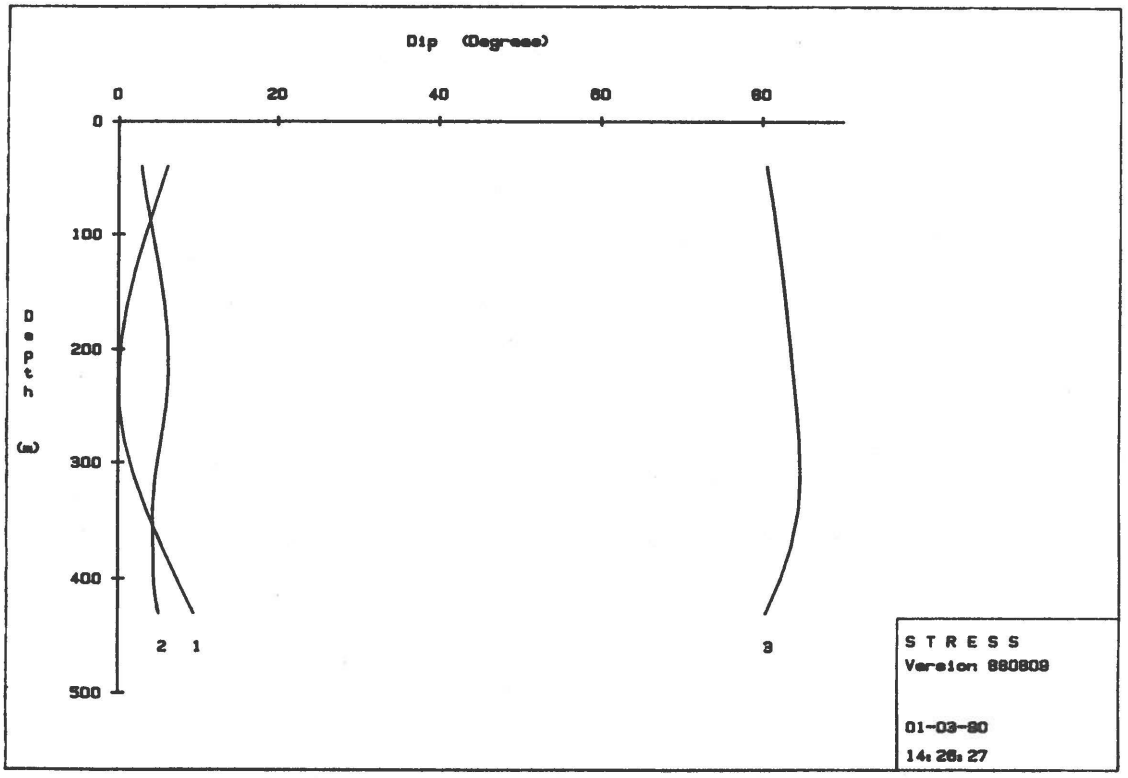


Fig.5.8. Dips of the principal stresses (3-D analysis).

Two important conclusions can be drawn from the three-dimensional treatment of the data:

- The stresses are oriented in the vertical and horizontal plane.

- The vertical stress is the minimum principal stress down to approximately 430 m depth.

No conclusion can be drawn from the three-dimensional HTPF analysis regarding the magnitudes and directions of the stresses due to the variation in obtained results between different input data sets that were applied. The variation may be a result of a non-linear stress field; as a data point is excluded or added it has a strong influence in case of a non-linear behaviour with depth. It may also be a result of non-successful field tests although they were interpreted as being successful.

6 COMPARISON OF RESULTS

The hydraulic fracturing measurements were evaluated in four different ways:

a) Classical approach and using T_{app} as tensile strength value; first breakdown method.

b) Classical approach and using T_f as tensile strength value; second breakdown method.

c) The method that takes into account the influence of the vertical and radial stresses acting at the borehole wall by using the Hoek and Brown failure criterion. The emirical constant m in the failure criteria was determined from laboratory tests on core samples.

d) Same as c) except for that the m-value was determined by back calculation from eq. (9b) where T_{app} was used as the tensile strength.

As was concluded in section 4.3.3 the authors adopt the evaluation method named the second breakdown method.

For the injection tests on preexisting fractures the two-dimensional solution obtained proved to be stable, whereas the three-dimensional calculation gave different solutions depending on which data points that were selected. However, despite the scatter in the 3-D solutins, the principal stresses showed to be oriented in the vertical and horizontal planes. The comparison of results in the following sections are therefore made between those obtained by the second breakdown method (hydraulic fracturing) and those obtained by the two-dimensional HTPF solution.

6.1 Orientations

The hydrofracturing measurements gave an average orientation of N-S (6 impressions) for the maximum horizontal stress, σ_H, and the HTPF method gave N37°W. As can be seen in Fig. 6.1 the individual data points for hydrofracturing orientations are rather scattered. Added in the figure are also the orientations obtained by sleeve fracturing, which gave the same orientation as the HTPF method. We then recall that the majority of induced fractures from laboratory hydraulic fracturing tests went in the direction of the existing foliation planes. Further, we recall that the orientation of the foliation planes in-situ was determined to be steeply dipping and striking N-S. Since there is a clear discrepancy in orientation of σ_H between the two methods, plus that the sleeve fracturing results indeed favour the orientation obtained by the HTPF method, it is reasonable to belive that the hydrofracturing induced fractures have been influenced by the existing planes of foliation and therefore do not reflect the true orientation of the maximum horizontal stress, σ_H.

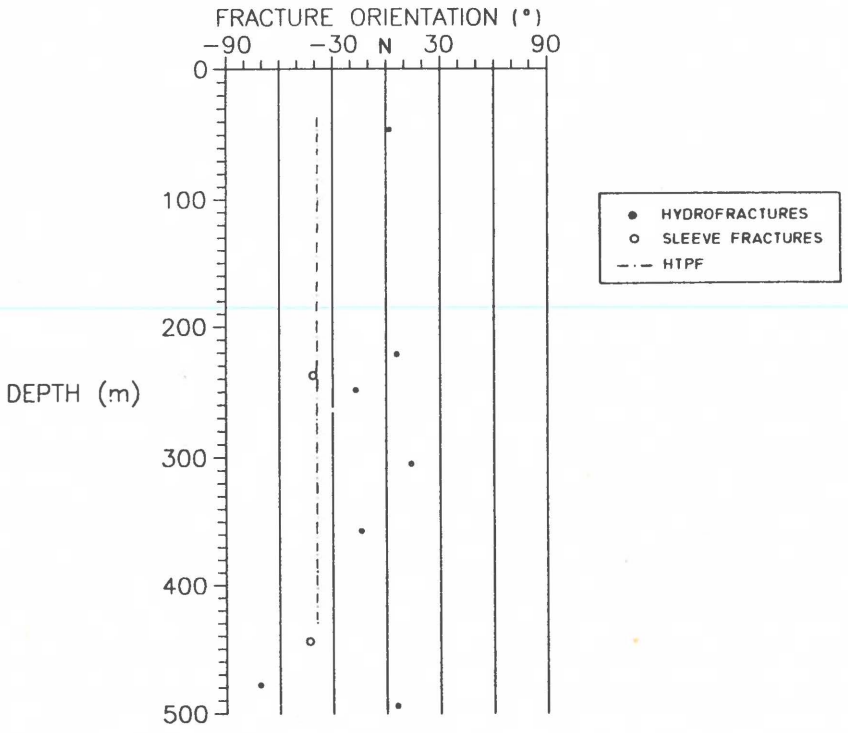


Fig. 6.1. Orientation of the maximum horizontal stress determined by hydrofracturing, HTPF method and sleeve fracturing.

6.2 Magnitudes

Fig. 6.2 shows the maximum and minimum horizontal stress determined by hydrofracturing measurements and the HTPF method. It can be seen that there is good agreement for the minimum horizontal stress, σ_h where the HTPF determined σ_h has a slightly less gradient. For the maximum horizontal stress, σ_H the difference is larger, being about 3 MPa at 430 m depth.

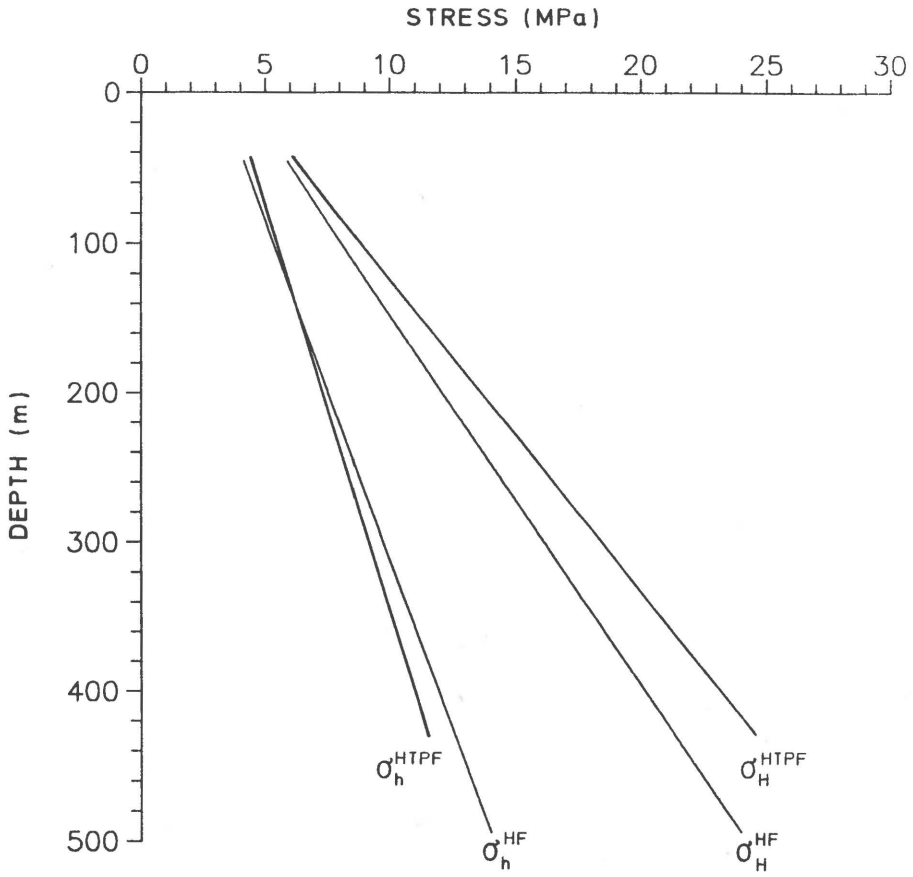


Fig. 6.2. Horizontal stresses as function of depth, Luleå.

It should be kept in mind, however, that the hydrofracturing induced fractures were initiated in directions that has been concluded are not aligned with the direction of the maximum horizontal stress. Therefore, comparison of the magnitudes can only be done under the assumption that the hydrofractures have turned and changed to the direction of the maximum horizontal stress as they were propagated out in the rock mass. Interestingly to see, there is some evidence that a reorientation of hydrofractures have occured. Looking at the orientations of the

hydrofractures at 477.8 m and 494.2 m, Fig. 6.1, we see that it differs 77° between them. If we then study Fig. 4.4, the difference in magnitude between the two measuring points is only 0.1 MPa. The only concluson that can be drawn from this is that one or both fractures reorientated as they were propagated, and ended up in planes with the same direction.

7 DISCUSSION AND FUTURE DEVELOPMENT

The measurements in LuH were the third, in Sweden, where both hydraulic fracturing and hydraulic tests on preexisting fractures were applied in the same borehole. This project is though the most extensive where the stress state has been independently evaluated from each method without knowing the results from the other.

The mesurements were conducted using identical field equipment for both methods. The field work required to collect data for the HTPF method is greater than what is needed for the hydrofracturing method. To locate a single joint with the downhole instruments is more time consuming than finding fracture-free sections. Besides, a core log which mostly is used to select fractures to be tested do not always match perfectely to what is found in the borehole wall. It might happen that fractures that have been logged as mechanically induced turns out to be natural and vice versa. This phenomena is of course a problem for both methods, but is more serious for the HTPF method since alternative single joints with similar strikes and dips have to be located.

The pump tests are more time consuming for HTPF. This is due to the lower flow rates applied for this method. One test point takes approximately an extra hour to complete. The HTPF method has been improved after the development of a personal computer program to evaluate the stress field, as on-site evaluation minimizes the risk of finishing the field work whitout having enough data to determine the stresses. However, comparing the methods, the HTPF technique requires a certain number of data points to evaluate the stress field, whereas the hydrofracturing method theoretically offers the possibility to determine the stresses at a point with only one successful test.

The evaluation procedure is also more time consuming for the HTPF method. This is not of great concern but it requires more time to interprete the field information.

The HTPF method is solely based on the measurement of the normal stress acting across fracture planes with different strikes and dips. The hydrofracturing method is based both on the normal stress, the strength of the rock and in some cases also the pore pressure. The normal stress is equal to the so-called shut-in pressure and is well understood and defined. The two other parameters are not that well defined. For Swedish rock we neglect the pore pressure and consider the rock as being impermeable during the time of pressurization.

As have been discussed in previous sections different approaches were applied to obtain reliable data on the tensile strength of the rock. The experience from 7 years of hydrofracturing measurements show that the second breakdown hydraulic fracturing method gives the most reliable information about the stress magnitude.

Stress discontinuities caused by for instance fracture zones can be detected by both measurement methods. If such a stress discontinuity is to be detected by hydraulic fracturing measurements, only a few measurements above and below the fracture zone should be needed, dependent on how distinct the stress discontinuity is. To obtain reliable information on stress versus depth above and below the zone , this requires about 5-7 measuring points on each side. To obtain the same information using the HTPF method it requires stress analyses above and below the discontinuity which in turn means, for 2-D analyses, that 8-10 reliable measuring points must be obtained on each side of the stress discontinuity.

If hydraulic fracturing rock stress measurements should be done in a rock type where marked foliation planes exist, it is recommended to carefully check the orientation of induced hydrofractures against the strike of the foliation planes. If a correlation exists between the orientation of the hydrofractures and the strike of the foliation planes one should be prepared to instead conduct the stress measurements according to the HTPF method. Such a correlation indicates that the foliation planes

represent weakness planes and hydraulic fracturing is then inapplicable. On the other hand, if no correlation exists, hydraulic fracturing should be preferred since the method is more rational.

The hydrofracturing unit at Luleå University of Technology has undergone continuous development from the start of the measurements. The latest contribution to improve and modernize the equipment is the computer based measuring system. All gauge signals of interest during the measurements are now recorded and stored on a personal computer. The system allows for real-time plotting of the information on the screen. The next step is to implement an evaluation procedure for the hydrofracturing field data to allow for on site evaluation of the stress magnitudes.

8 CONCLUSIONS

- The orientation of the maximum horizontal stress, from measurements in borehole LuH, is approximately N40°W, as determined by the HTPF method and sleeve fracturing tests.

- The induced hydrofractures were influenced by the steeply dipping foliation planes in the rock mass, and do therefore not reflect the orientation of the maximum horizontal stress.

- The hydrofracturing second breakdown method and 2-D HTPF method give similar results for the magnitudes of the horizontal stresses. At 400 m depth the stress magnitudes for σ_H and σ_h are about 21.5 MPa and 11.5 MPa, respectively.

- The lack of reliable strength data for the rock mass is the major difficulty when applying the Hoek and Brown criteria on hydrofracturing data.

- The three-dimensional HTPF analysis shows that the principal stresses are oriented in the vertical and horizontal planes.

- The orientation of the maximum horizontal stress agrees with the direction of the velocity trajectories from the mid-atlantic ridge push.

- The vertical stress, measured by shut-in pressures on two subhorizontal fractures, is in the range of the overburden stress, ρgz.

- The HTPF method still suffers of being time consuming compared to hydraulic fracturing. To reduce the time needed for field measurements, more accurate in-the-hole instruments are needed for the location of single preexisting fractures.

- 8-10 reliable measuring points are required to perform a

two-dimensional stress analysis. If a stress discontinuity intersects the depth interval where meaurements are conducted the number of measuring points must be doubled, evenly spread above and below the discontinuity.

- If time and cost are deciding factors the HTPF method should replace the hydrofracturing technique only in cases where none of the principal stresses are expected to be parallel to the borehole axis or when marked weakness planes exist in the rock mass.

9 ACKNOWLEDGEMENTS

Mr. Arne Torikka and Mr. Hans Klasson assisted during the field measurements. Their work is greatly appreciated. This work was supported by the Swedish Natural Science Research Council under contract E-EG 3447-140 and the Swedish Rock Engineering Research Foundation within project BeFo 211.

10 REFERENCES

Bjarnason, B. 1986. Rock stress measurements in borehole 4, Stajsås, Siljan area,Sweden. Centek/University of Luleå, Preliminary report, 11 p.

Bjarnason, B. and Stephansson, O. 1986. Hydraulic fracturing rock stress measurements in borehole Gi-1 Gideå study site, Sweden. Technical report 86-11. Swedish Nuclear Fuel and Waste Management Co., Stockholm, Sweden, 44 p.

Bjarnason, B. and Raillard, G. 1987. Rock stress measurements in borehole V3. Internal Report, Stripa Project 87-13. Swedish Nuclear Fuel and Waste Management Co., Stockholm, Sweden, 40 p.

Bjarnason, B. and Torikka, A. 1989. Field instrumentation for hydrofracturing stress measurements. Documentation of the 1000 m hydrofracturing unit at Luleå University of Technology. Technical report 89-17. Swedish Nuclear Fuel and Waste Management Co., Stockholm, Sweden, 24 p.

Cornet, F.H. 1981. Interpretation of hydraulic injection tests for in-situ stress determination. Proc. of Workshop on Hydraulic Fracturing Rock Stress Measurements, Dec. 2-5, Monterey, pp. 149-158.

Cornet, F.H. and Valette, B. 1984. In situ stress determination from hydraulic injection test data. Journal of Geophysical Research, Vol. 89, No. B13, pp 11,527-11,537.

Doe, T.W., Ingevald, K., Strindell, L., Leijon, B., Hustrulid, W., Majer, E. and Carlsson, H. 1983. In-situ stress measurements at the Stripa mine, Sweden. Report LBL-15009, SAC44. Swedish-American Cooperative Program on Radioactive Waste Storage in Mined Caverns in Crystalline Rock, 251 p.

Doe, T.W. 1987. A comparison of hydraulic fracturing and hydraulic jacking stress measurements. 28th U.S. Symp. on Rock

Mechanics, University of Arizona, Tuscon.

Hubbert, M.K. and Willis, D.G. 1957. Mechanics of hydraulic fracturing. Trans. A.I.M.E., 210, pp. 153-168.

Kirsch, G. 1898. Die theorie der elastizitat und die bedurfnisse der festigkeitslehre. Veit. Ver. Deut. Ing. 42, pp. 797-807.

Lilljequist, R. 1980. The geological development of southeastern Norrbotten, based on the Precambrian stratigraphy of the Luleå area. Geologiska Föreningens i Stockholm Förhandlingar, Vol. 102, Pt. 2, pp. 181-183. Stockholm. ISSN 0016-786X.

Ljunggren, C. and Raillard, G. 1987. Rock stress measurements by means of hydraulic tests on pre-existing fractures at Gideå test site, Sweden. Int. J. Rock Mech. Min. Sci. & Geomech. Abstr., Vol. 24, No. 6, pp. 339-345.

Ljunggren, C. 1987. Determination of virgin rock stresses by fracturing methods. Licentiate Thesis 1987:10L, Luleå University of Technology, Sweden.

Ljunggren, C., Amadei, B. and Stephansson, O. 1988. Use of the Hoek and Brown failure criterion to determine in-situ stresses from hydraulic fracturing measurements. Proc. of Conference on Applied Rock Engineering (CARE '88), Newcastle upon Tyne, England, Jan. 6-8, pp. 133-142.

Ludvig, B. 1981. A description of the rock body around the rock heat store at the University of Luleå. Internal Report BM 1981:10, Div. of Rock Mechanics, Luleå University of Technology, Sweden. (in Swedish)

Paris, P. and Sih, G. 1965. Stress analysis of a crack. In: Fracture Toughness and its testing. American Society of testing and Materials Special Publications 381, pp. 30-83.

Röshoff, K. and Norin, J. 1982. Borehole documentation of the boreholes in the rock heat store. Internal report BM 1982:10, Div. of Rock mechanics, Luleå University of Technology, Sweden. (in Swedish)

Stephansson, O. and Ångman, P. 1986. Hydraulic fracturing stress measurements at Forsmark and Stidsvig, Sweden. Bull. Geol. Soc. Finland, 58, Part 1, pp. 307-333.

Thorsager, P. 1987. Dokumentation av kärnborrhålet vid LuH med Rockdisc. M.S. Thesis 1987:159E, Luleå University of Technology, Luleå, (in Swedish)

APPENDIX 1

Table A1. Pressure data from borehole LuH, Luleå

Depth (m)	P_{b1} (MPa)	P_{b2} (MPa)	P_{b3} (MPa)	P_{b4} (MPa)	P_{s1} (MPa)	P_{s2} (MPa)	P_{s3} (MPa)	P_{s4} (MPa)
46.0	9.55	5.8	5.7	5.3	4.3	3.9	3.6	3.3
98.6	13.0	9.1	8.8	8.6	6.0	5.4	4.8	4.2
138.3	16.3	10.6	10.6	10.2	7.6	7.4	7.2	6.8
221.4	13.8	9.8	9.2	9.0	9.3	9.3	9.4	9.3
248.6	18.1	11.8	10.9	10.8	9.1	9.0	8.7	8.1
304.8	21.8	11.3	10.9	10.7	9.9	9.1	9.0	9.0
323.3	23.0	13.1	12.7	0	10.1	9.9	9.1	0
357.0	18.6	15.6	14.6	13.6	12.0	11.6	11.4	10.9
477.8	24.0	16.8	16.8	16.8	14.7	14.4	14.0	13.6
494.2	24.6	19.8	18.8	19.0	15.6	14.8	13.9	13.2

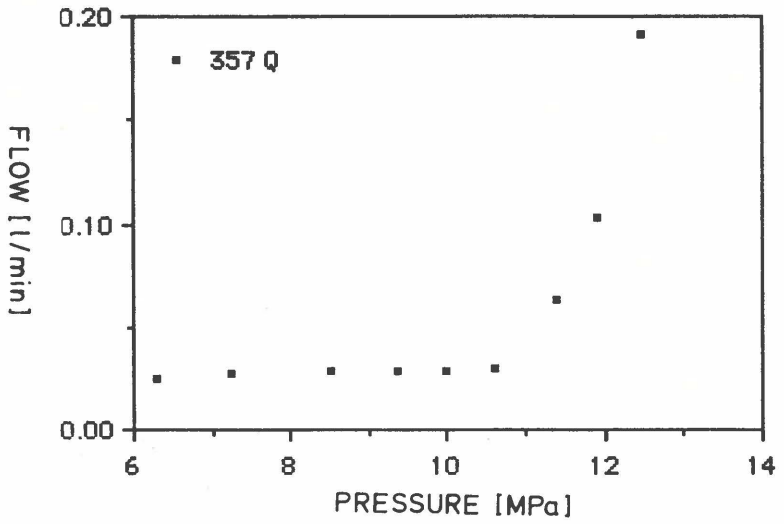
Table A2. Fracture orientations in borehole LuH, Luleå

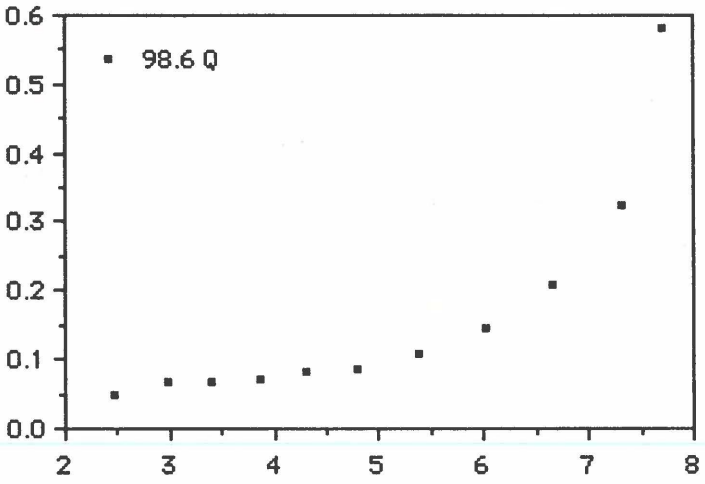
Depth (m)	F1°	F2°	F2° - F1°	σ_H°	Comments
46.0	1	183	182	N2E	+
72.4					
81.3					
98.6	105	270	165	N83W	(+)
138.3	129	296	167	N58W	(+)
175.6					
221.4	2	190	188	N6E	+
248.6	161	346	185	N17W	+
277.0					
288.6					
304.8	10	199	189	N14E	+
323.3	0	184	184	N2E	(+)
357.0	153	358	205	N14W	+
372.1					
402.3					
469.4					
477.8	112	285	173	N71W	+
494.2	6	186	180	N6E	+

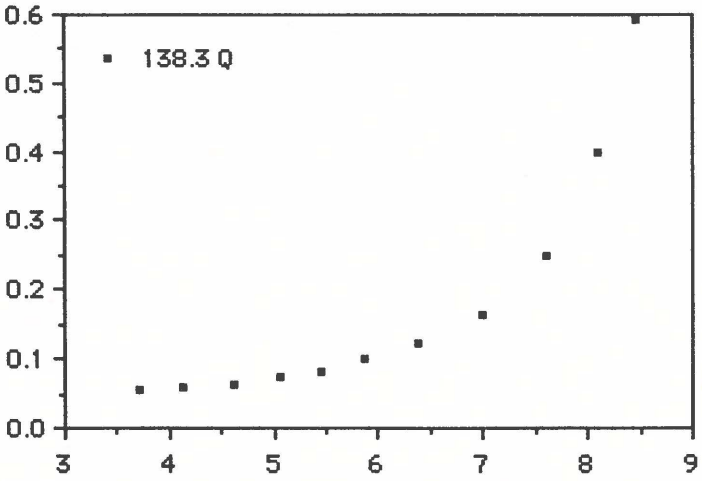
F1°, F2° = The orientation of each fracture measured clockwise from zero at N (360° circle). σ_H° = Orientation of maximum horizontal stress. + = Two vertical or near vertical fractures. (+) = Vertical fractures of uncertain origin.

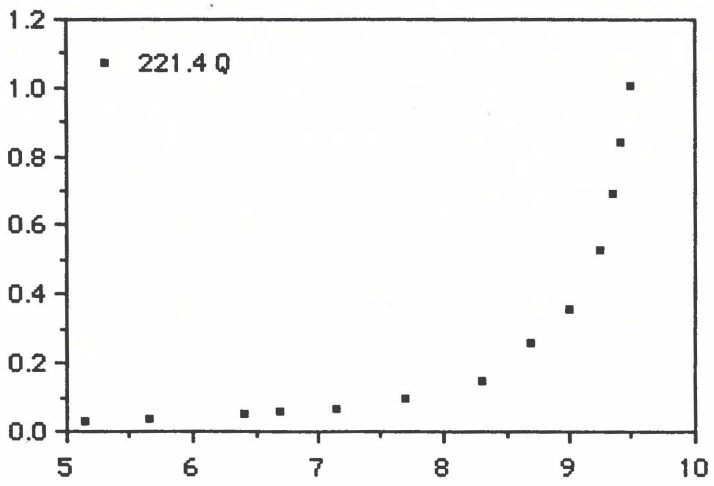
APPENDIX 2

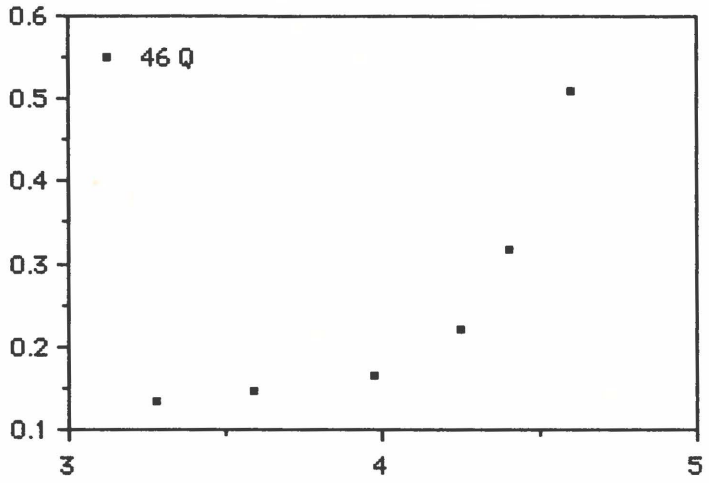
Pressure-flow diagrams for the determination of the hydraulic jacking pressure

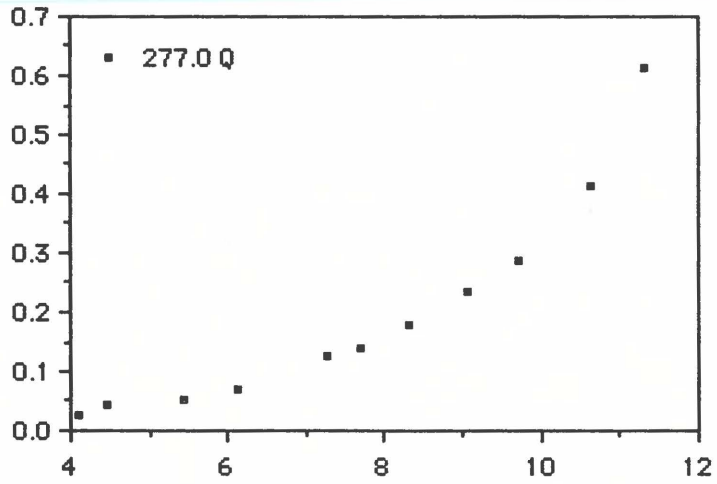


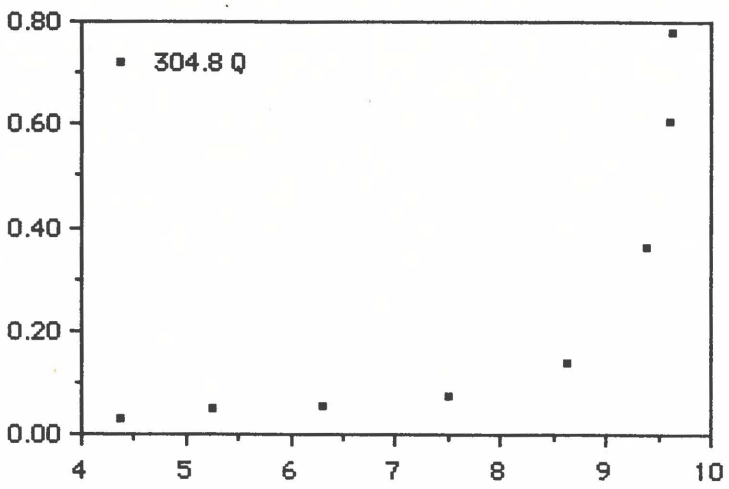


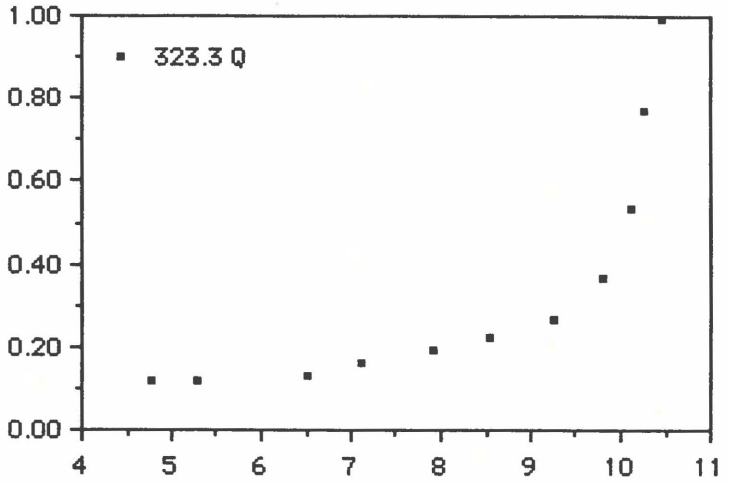


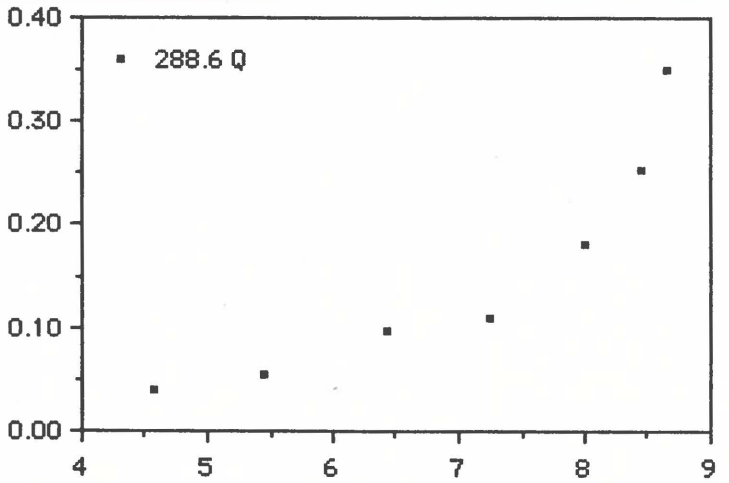

221.4 Q
1.2
1.0
0.8
0.6
0.4
0.2
0.0
5
6
7
8
9
10

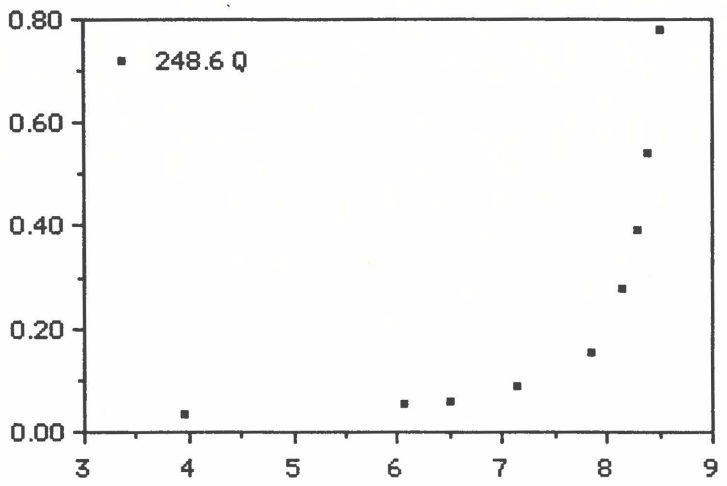

46 Q
0.6
0.5
0.4
0.3
0.2
0.1
3
4
5

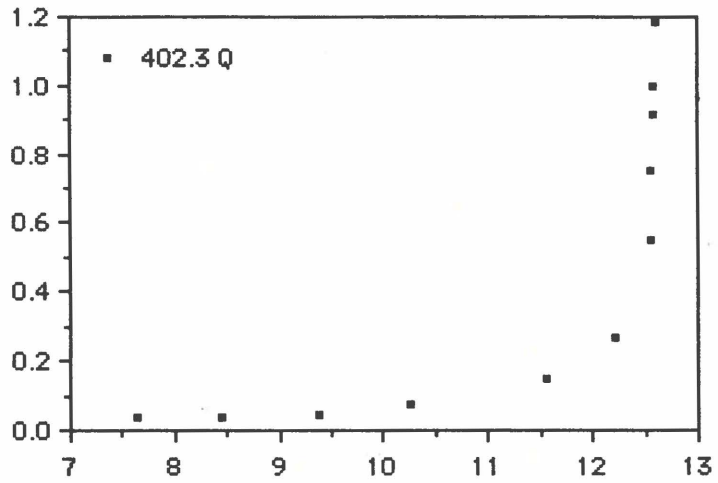

277.0 Q
0.7
0.6
0.5
0.4
0.3
0.2
0.1
0.0
4
6
8
10
12

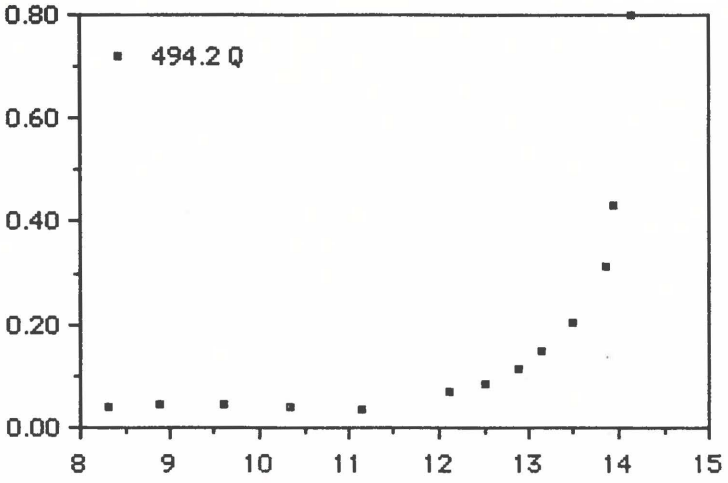

304.8 Q
0.80
0.60
0.40
0.20
0.00
4
5
6
7
8
9
10

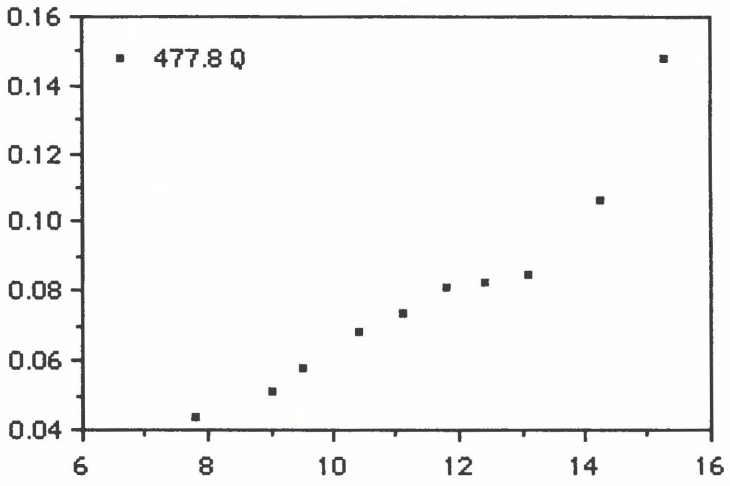

323.3 Q
1.00
0.80
0.60
0.40
0.20
0.00
4
5
6
7
8
9
10
11

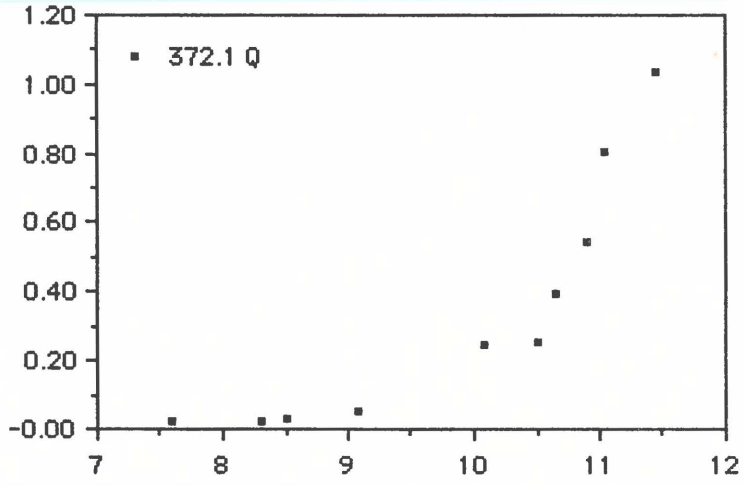

288.6 Q
0.40
0.30
0.20
0.10
0.00
4
5
6
7
8
9

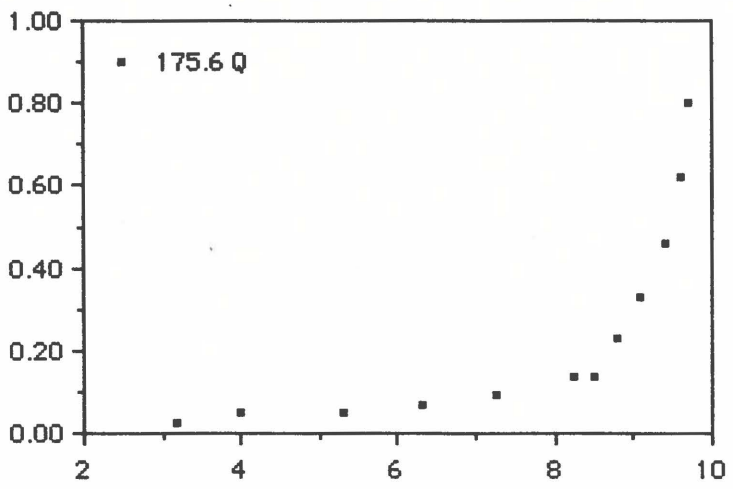

248.6 Q
0.80
0.60
0.40
0.20
0.00
3
4
5
6
7
8
9


402.3 Q
1.2
1.0
0.8
0.6
0.4
0.2
0.0
7
8
9
10
11
12
13


494.2 Q
0.80
0.60
0.40
0.20
0.00
8
9
10
11
12
13
14
15

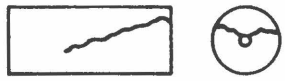
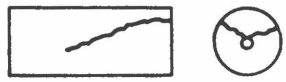
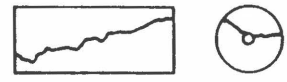

477.8 Q
0.16
0.14
0.12
0.10
0.08
0.06
0.04
6
8
10
12
14
16


372.1 Q
1.20
1.00
0.80
0.60
0.40
0.20
-0.00
7
8
9
10
11
12

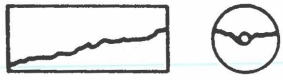

1.00
0.80
0.60
0.40
0.20
0.00
175.6 Q
2
4
6
8
10

APPENDIX 3

Table A3. Results from laboratory testing of tensile strength on core samples from borehole LuH, Luleå.

DEPTH [m]	P_i^c [MPa]	FAILURE MODE	COMMENTS
47.4	8.1		Gneiss Fracture paralell to the foliation
47.5	6.7		Gneiss Fracture paralell to the foliation
47.6	5.1		Gneiss Fracture paralell to the foliation
80.0	12.8		Gneiss Fracture paralell to the foliation Single fracture
80.1	12.2		Gneiss Fracture paralell to the foliation
80.2	9.0		Gneiss Fracture paralell to the foliation
183.7	13.3		Gneiss Fracture paralell to the foliation
183.8	10.4		Gneiss Fracture paralell to the foliation
183.9	8.5		Gneiss Fracture paralell to the foliation
288.4	14.7		Gneiss Fracture paralell to the foliation
288.5	13.1		Gneiss Fracture turned toward the foliation

cont. Table A3

DEPTH [m]	P_i^c [MPa]	FAILURE MODE	COMMENTS
288.6	11.6		Gneiss
289.1	14.3		Gneiss Fracture perpendicular to the foliation
289.2	13.8		Gneiss Fracture perpendicular to the foliation
289.3	15.4		Gneiss Fracture partly paralell to the foliation
371.5	12.2		Gneiss Fracture paralell to the foliation
371.6	13.6		Gneiss Fracture paralell to the foliation
463.5	14.1		Granite
463.6	16.4		Granite
463.7	17.5		Granite Symmetric